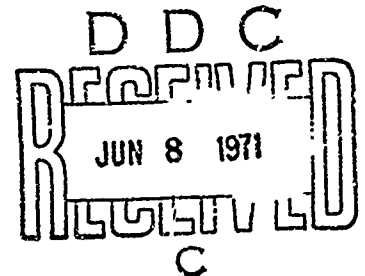AD724723

VORTEX INDUCED ROLLING MOMENTS ON CRUCIFORM MISSILES AT HIGH ANGLE OF ATTACK

by

Steven I. Kane

Engineering Laboratories
Boston University
110 Cummington Street
Boston, Massachusetts 02215

D D C

RECEIVED
JUN 8 1971
C

SCIENTIFIC REPORT NO. 3
March 1971

Prepared
for

AIR FORCE CAMBRIDGE RESEARCH LABORATORIES
AIR FORCE SYSTEMS COMMAND
UNITED STATES AIR FORCE
BEDFORD, MASSACHUSETTS 01730

64

Qualified requestors may obtain additional copies from the
Defense Documentation Center. All others should apply to
the Clearinghouse for Federal Scientific and Technical
Information.

DOCUMENT CONTROL DATA - R&D

(Security classification of title, body of abstract and indexing annotation must be entered when the overall report is classified)

1. ORIGINATING ACTIVITY (Corporate author)	2a. REPORT SECURITY CLASSIFICATION
Boston University Engineering Laboratories Boston, Massachusetts 02215	Unclassified
	2b. GROUP

3. REPORT TITLE

VORTEX INDUCED ROLLING MOMENTS ON CRUCIFORM MISSILES AT HIGH ANGLE OF ATTACK

4. DESCRIPTIVE NOTES (Type of report and inclusive dates)

Scientific   Interim

5. AUTHOR(S) (First name, middle initial, last name)

Steven I. Kane

6. REPORT DATE	7a. TOTAL NO. OF PAGES	7b. NO. OF REFS
March 1971	61	6

8a. CONTRACT OR GRANT NO.	9a. ORIGINATOR'S REPORT NUMBER(S)
F19628-68-C-0148	
b. PROJECT, TASK, WORK UNIT NOS. 7659-04-01	Scientific Report No. 3
c. DOD ELEMENT 62101F	9b. OTHER REPORT NO(S) (Any other numbers that may be assigned this report)
d. DOD SUBELEMENT 681000	AFCRL-71-0093

10. DISTRIBUTION STATEMENT

1-This document has been approved for public release and sale; its distribution is unlimited.

11. SUPPLEMENTARY NOTES	12. SPONSORING MILITARY ACTIVITY
TECH, OTHER	Air Force Cambridge Research Laboratories (LC) L.G. Hanscom Field Bedford, Massachusetts 01730

13. ABSTRACT

The problem of predicting the induced roll phenomena associated with finned missiles at high angles of attack has been approached by examining the interaction between the body wake vortex system and the finned surfaces of the missile. The application of the classic Blasius moment integral to this problem permits the independent evaluation of each singularity in the flow field which may contribute to the moments. This method is applicable to missiles employing fin schemes of any geometry and is used herein to analyze the induced roll of a typical cruciform missile configuration.

A computer program has been developed to generate numerical solutions utilizing those parameters which affect the magnitude and direction of the induced roll.

DD FORM 1473
1 NOV 65

14. KEY WORDS	LINK A		LINK B		LINK C	
	ROLE	WT	ROLE	WT	ROLE	W
Blasius Integral						
Cruciform Fin						
Finned Missiles						
Rolling Moment						
Vortex						

VORTEX INDUCED ROLLING MOMENTS ON CRUCIFORM MISSILES AT
HIGH ANGLE OF ATTACK

by

Steven I. Kane

Engineering Laboratories
Boston University
110 Cummington Street
Boston, Massachusetts 02215

SCIENTIFIC REPORT NO. 3
March 1971

Prepared
for

AIR FORCE CAMBRIDGE RESEARCH LABORATORIES
AIR FORCE SYSTEMS COMMAND
UNITED STATES AIR FORCE
BEDFORD, MASSACHUSETTS 01730

ABSTRACT

The problem of predicting the induced roll phe-
nomena associated with finned missiles at high angles of
attack has been approached by examining the interaction be-
tween the body wake vortex system and the finned surfaces
of the missile. The application of the classic Blasius
Moment Integral to this problem permits the independent
evaluation of each singularity in the flow field which may
contribute to the moments. This method is applicable to
missiles employing fin schemes of any geometry and is used
herein to analyze the induced roll of a typical cruciform
missile configuration.

A computer program has been developed to generate
numerical solutions utilizing those parameters which affect
the magnitude and direction of the induced roll.

TABLE OF CONTENTS

LIST OF SYMBOLS

a $(c^4 - R^4)^{1/4}$

b   Fin semi-span (see Fig. 1)

c $\sqrt{2(b^2 + R^4/b^2)}/2$ = radius of circle in the ξ plane (see Fig. 3)

c_{M_o} Rolling moment coefficient $\left(= \dfrac{M_o}{1/2 \, \rho U^2 b^2 L}\right)$

c_Γ Vortex strength coefficient $\left(= \dfrac{\Gamma}{2\pi R U}\right)$

$F(\xi)$ $f(\xi) w^2(\xi)$

$f(\xi)$ $\dfrac{z}{dz/d\xi}$

$g(\xi)$ See Appendix A

H See Equ. (32)

$h(r)$ See Equ. (27)

$I^m_{\xi_o}$ Blasius integral around pole of order m at ξ_o (see Equ. (8))

$I_{I,II}$ Blasius integral around branch cut between ξ_I and ξ_{II}

$I_{VII,VI}$ Blasius integral around branch cut between ξ_{VII} and ξ_{VI}

i Unit pure imaginary number

List of Symbols (continued)

J	$\sqrt{C^2 + R^2}/2$	(see Equ. (18))
K	$\sqrt{C^2 - R^2}/2$	(see Equ. (19))
L	Chord length of fin	
M	Cross flow Mach number	
M_O'	Rolling moment/unit length of fin	
M_O	Rolling moment	
m	Order of pole	
q	Dynamic pressure $= \frac{1}{2}\rho V_\infty^2$	
R	Radius of cylindrical body (see Figure 1)	
r	Polar coordinate (see Figs. 5 and 6)	
U	Cross flow velocity $= V_\infty \sin \alpha$	
u	Velocity in x direction or real component of complex velocity	
V_∞	Free stream velocity	
v	Velocity in y direction or imaginary component of complex velocity	
W	Complex velocity potential	

List of Symbols (continued)

w   Complex velocity=$u-iv$

x   Fin axis in tail body plane (see Figs. 1 and 2)

y   Axis perpendicular to x axis in tail body plane (see Figs. 1 and 2)

z   Complex plane (see Fig. 2)

α Angle of attack of missile

β Residue (see Equ. (7))

Γ Vortex strength

γ Arbitrary circulation around body

ϵ Radius of contour about branch point (see Figs. 5 and 6)

ξ Complex plane of the circle (see Fig. 3)

ξ_0 Position of a pole in the ξ plane

ξ_0' Position of stagnation point on the circle in the ξ plane (see Appendix B)

$\xi_I, \xi_{II},$--Branch points in the ξ plane

$\eta(r)$ See Equ. (26)

List of Symbols (continued)

Θ Polar coordinate (see Figs. 5 and 6)

Θ_o Argument of ξ'_o (see Appendix B)

P See Equ. (42)

P See Equ. (45)

ρ Fluid density

$\dot{\tau}$ See Equ. (41)

ϕ Roll angle (see Fig. 1)

ψ Stream function (imaginary part of W)

SECTION I.   Introduction

Rockets and missiles employing fins of cruciform arrangement have been found to develop anomalous aerodynamic rolling moments which are functions of, among other things, the angle of attack, the bank orientation of the wings and Mach number. These rolling moments tend to upset the stability by rolling the missile, and unless they are counteracted by roll-control measures, the actual flight path control accuracy is apt to deteriorate at a crucial time. It is generally accepted that the absolute magnitude of the induced rolling moment is of primary concern.

Induced roll phenomena, which could be significant for some configurations at low angles of attack, become of increased importance as the angle-of-attack range is extended for the purpose of increased maneuverability. The source of high angle of attack problems has been found to be associated with body-wing or body-tail interference.

Without the mitigation of these induced rolling moments, high-angle-of-attack maneuvers in some cases may be precluded or in other cases result in increased control system complexity or increased size of the wing surfaces. Such alternatives usually result in overall performance degradations.

The possible major sources of anomalous induced rolling moments for typical rocket configurations were discussed and evaluated in Ref. 1. The magnitude of some of these rolling moments have been found to be negligible compared to the induced rolling moments observed from experimental investigations. Strong evidence is available (Ref. 2) to support the argument that the interaction of

the wing or tail surfaces with the vortex system generated
by the body is largely responsible for the induced rolling
moment phenomenon.

The vortices formed in the wake of a body affect
the attached lifting surfaces by altering the local flow
characteristics--i.e., angle of attack, Mach number, static
pressure, etc.--across the span. The variations in the
magnitude and spanwise distribution of the panel normal
forces, which are produced by these changes in local flow
characteristics, are, therefore, functions of both the
strength of the vortices and the geometry of the wing-
vortex system. Consequently, comprehension and prediction
of the effects of wing-vortex interactions must depend
critically on the description of the vortex system itself.
Fortunately, experimental data are available (Ref. 3) which
describe the wake vortex system generated by the body of
the wing-body configuration considered in the present study.
These vortex data eliminate the additional complexity of
relying on theoretical estimates of the vortex system and
are used herein as a basis for analysis.

It should be noted that the Blasius moment inte-
gral has been recently applied (see Ref. 1) in evaluating
the induced roll of planar missile configurations.

SECTION II.   General Formulation of the Problem

In order to simplify the problem we will assume
(as was done in Ref. 1 for the planar model) that the flow
is steady; incompressible, and inviscid. The assumption of
negligible missile roll rate will allow for the steady flow
condition.

A typical body-tail configuration utilizing four
equally-spaced rectangular fins will serve as our model for
analysis; (as will be shown later the fin can be of any de-
sired shape such as triangular, trapezoidal, etc.). The
model in the cross-flow plane (Fig. 1) shows the cross flow
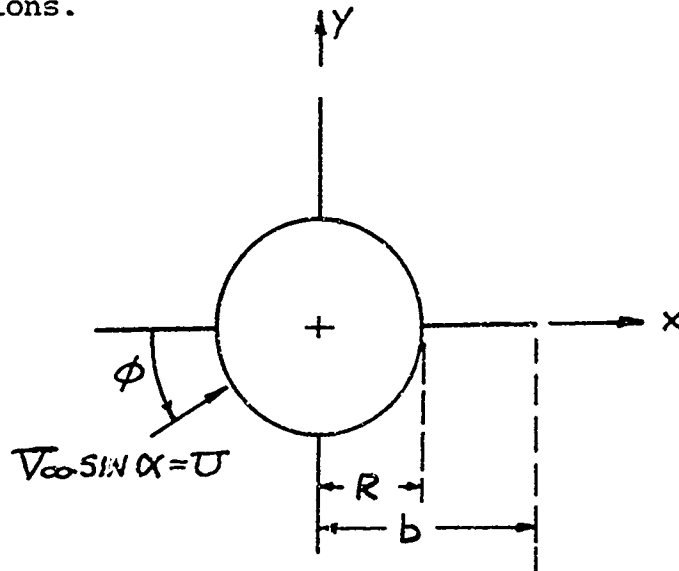velocity, U, the missile roll attitude, ϕ, and pertinent
model dimensions.

Figure 1.   The Cross-Flow Plane

We may now represent the complex potential for
this flow in the Z plane (Fig. 2) by $W(Z)$ where the two
body vortices are shown relative to the fins and the

cross-flow velocity U. Because of the missile roll the
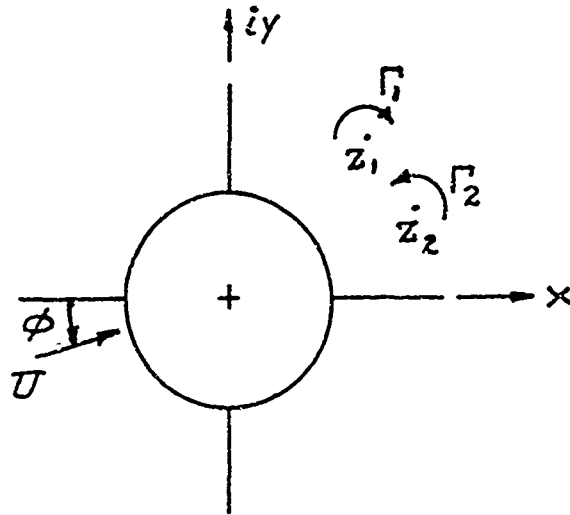vortices are not necessarily symmetric or of equal strengths.

Figure 2. The Z Plane

For steady state rolling moments about the origin
the Blasius moment integral is given as

$$M_o' = -Re\frac{\rho}{2}\oint z\left(\frac{dW}{dz}\right)^2 dz \tag{1}$$

where the contour is along the outside of the body surface.

The analysis can be considerably simplified if
the configuration in the Z plane is conformally mapped into
a circle. The mapping procedure for the cruciform shape
can be found in Ref. 4. Thus the ξ plane (Fig. 3) repre-
sents the mapping of the missile contour into a circle of
radius c. (Note that the magnitude and direction of the

cross-flow velocity and the magnitude of the two body
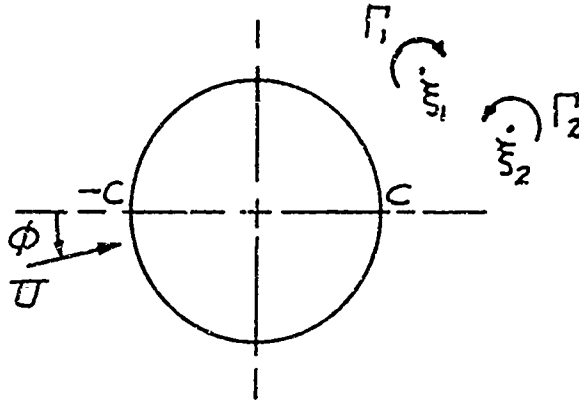vortices are unaltered by the mapping.*)

Figure 3. The ξ plane

The relationships between corresponding points in both
planes are

$$\xi = \pm \frac{1}{\sqrt{2}} \sqrt{\left(Z^2 + \frac{R^4}{Z^2}\right) \pm \sqrt{\left(Z^2 + \frac{R^4}{Z^2}\right)^2 - 4C^4}} \tag{2a}$$

and

$$Z = \pm \frac{1}{\sqrt{2}} \sqrt{\left(\xi^2 + \frac{C^4}{\xi^2}\right) \pm \sqrt{\left(\xi^2 + \frac{C^4}{\xi^2}\right)^2 - 4R^4}} \tag{2b}$$

where $\quad C \equiv \sqrt{2\left(b^2 + \frac{R^4}{b^2}\right)} \Big/ 2 .$

---

*See Appendix A of Reference 1.

The choice of signs in (2a) and (2b) is based on the following rules:

> (1) The "outside" plus and minus signs hold for the right half and the left half of the z or ξ planes, respectively.

> (2) The "inside" plus and minus signs are chosen accordingly to insure that the exterior of the body maps to the exterior of the circle.

The reader is referred to Ref. 1 (p. 15) for the derivation of the complex potential $W(\xi)$ which was obtained in the following form:

$$W(\xi) = U\left(e^{-i\phi}\xi + e^{i\phi}\frac{c^2}{\xi}\right)$$
$$+ \frac{i\Gamma_1}{2\pi}\left[ln(\xi-\xi_1) - ln\left(\frac{c^2}{\xi} - \bar{\xi}_1\right)\right] \tag{3}$$
$$- \frac{i\Gamma_2}{2\pi}\left[ln(\xi-\xi_2) - ln\left(\frac{c^2}{\xi} - \bar{\xi}_2\right)\right] + \frac{i\gamma}{2\pi}ln\frac{\xi}{c}$$

where the velocity potential takes into account the possible presence of a Kutta condition by including an arbitrary votex of strength γ with center at the origin.

As shown in Ref. 1 (p. 16) the Blasius integral may also be expressed as

$$M_o' = -Re\,\frac{\rho}{2}\oint f(\xi)W^2(\xi)d\xi \tag{4}$$

where $\quad f(\xi) \equiv \dfrac{z}{dz/d\xi}$

and
$$W(\xi) \equiv \frac{dW}{d\xi} \quad .$$

The use of the expression for Z as a function of ξ (Equ. (2b)) and its first derivative

$$\frac{dZ}{d\xi} = \pm \frac{1}{\sqrt{2}} \left(\xi - \frac{C^4}{\xi^3} \right) \left[\frac{1 \pm \dfrac{\xi^2 + C^4/\xi^2}{\sqrt{(\xi^2 + C^4/\xi^2)^2 - 4R^4}}}{\sqrt{(\xi^2 + C^4/\xi^2) \pm \sqrt{(\xi^2 + C^4/\xi^2) - 4R^4}}} \right]$$

gives, after algebraic expansion,

$$f(\xi) = \frac{\xi}{(\xi^2 + C^2)(\xi^2 - C^2)} \left[\xi^4 + C^4 \mp \frac{4R^4 \xi^4}{\sqrt{(\xi^4 + C^4)^2 - 4R^4 \xi^4} + (\xi^4 + C^4)} \right] \quad . \tag{5}$$

The reader is referred to Appendix A for a list of derivatives of $f(\xi)$.

The expression for $W^2(\xi)$ can be found in Ref. 1 (p. 17) where the singularities are shown to be poles, located at

$$\xi = 0, \; \xi_1, \; \xi_2, \; \frac{C^2}{\xi_1}, \; \frac{C^2}{\xi_2} \quad .$$

(The poles at $\dfrac{C^2}{\xi_1}$ and $\dfrac{C^2}{\xi_2}$ are inside the circle.) Since ξ_1 and ξ_2 are exterior to the circle $\xi = C$, they need not be accounted for as contributions to the integral.

The remaining singularities of the integrand all lie on the circle and are due to $f(\xi)$ (Equ. (5)). These are poles at $\xi = \pm c$ and $\xi = \pm ic$ and branch points where the

square root radical vanishes

$$\left(\xi^4 + C^4\right)^2 - 4R^4\xi^4 = 0$$

or

$$\xi^4 + C^4 = \pm 2R^2\xi^2 .$$

Rearranging, we have

$$\xi^4 \mp 2R^2\xi^2 + C^4 = 0$$

and

$$\xi^2 = \pm R^2 \pm \sqrt{R^4 - C^4} .$$

Thus branch points are located at

$$\xi = \pm\sqrt{\pm R^2 \pm ia^2}$$

where

$$a^2 \equiv \sqrt{C^4 - R^4} .$$

That is, eight branch points appear at

$$\left.\begin{aligned}
\xi_I &= \frac{-1}{\sqrt{2}}\left(\sqrt{C^2 - R^2} - i\sqrt{C^2 + R^2}\right) \\
\xi_{II} &= \frac{1}{\sqrt{2}}\left(\sqrt{C^2 - R^2} + i\sqrt{C^2 + R^2}\right) \\
\xi_{III} &= \frac{1}{\sqrt{2}}\left(\sqrt{C^2 - R^2} - i\sqrt{C^2 + R^2}\right) \\
\xi_{IV} &= \frac{-1}{\sqrt{2}}\left(\sqrt{C^2 - R^2} + i\sqrt{C^2 + R^2}\right) \\
\xi_{V} &= \frac{-1}{\sqrt{2}}\left(\sqrt{C^2 + R^2} - i\sqrt{C^2 - R^2}\right) \\
\xi_{VI} &= \frac{1}{\sqrt{2}}\left(\sqrt{C^2 + R^2} + i\sqrt{C^2 - R^2}\right) \\
\xi_{VII} &= \frac{1}{\sqrt{2}}\left(\sqrt{C^2 + R^2} - i\sqrt{C^2 - R^2}\right) \\
\xi_{VIII} &= \frac{-1}{\sqrt{2}}\left(\sqrt{C^2 + R^2} + i\sqrt{C^2 - R^2}\right)
\end{aligned}\right\} \tag{6}$$

9

These are all on the circle since in each case

$$|\xi| = \left(\left(R^4 + a^4\right)^{1/2}\right)^{1/2} = \left(C^4\right)^{1/4} = C \;.$$

SECTION III. Contour Integral Evaluation

The procedure for evaluation of the poles is shown in Ref. 1 (p. 20). Thus, if a complex function has a pole of order m at $\xi = \xi_0$, then its residue there is

$$\beta = \lim_{\xi \to \xi_0} \frac{1}{(m-1)!} \frac{d^{(m-1)}}{d\xi^{(m-1)}} \left[(\xi - \xi_0)^m F(\xi) \right] . \tag{7}$$

Referring to Equ. (4), a contour around a pole of order m of the Blasius integral located at $\xi = \xi_0$ can be expressed as

$$I_{\xi_0}^m = -Re\,\pi i\,\rho\,\beta(\xi_0, m) \tag{8}$$

where β can be defined as

$$F(\xi) \equiv f(\xi) W^2(\xi) \tag{9}$$

in Equ. (7).

For the simple poles at $\xi = c$ the integral is

$$I_c' = -Re\,\pi i\,\rho \lim_{\xi \to c} \left[(\xi - c) \frac{\xi W^2(\xi)}{(\xi^2 - c^2)(\xi^2 + c^2)} \left(\mp \frac{\xi^4 + c^4}{\sqrt{(\xi^4 + c^4)^2 - 4R^4\xi^4} \pm (\xi^4 + c^4)} \right) \right]$$

$$= -Re\,\pi i\,\frac{\rho}{2} \left[c^2 \mp \frac{R^4}{a^2 \pm c^2} \right] W^2(c) .$$

Similarly, for the pole at $\xi = -c$ the integral is

$$I_{-c}' = -Re\,\pi i\,\frac{\rho}{2} \left[c^2 \mp \frac{R^4}{a^2 \pm c^2} \right] W^2(-c) .$$

The total contribution due to the poles at c and $-c$ is thus

$$I'_c + I'_{-c} = Re\,\pi i \oint_{\frac{1}{2}} \left[\frac{\pm R^4}{a^2 \pm c^2} - c^2 \right]\left[w^2(c) + w^2(-c) \right] \quad . \tag{10}$$

Since $Re\,w(c) = Re\,w(-c) = 0$, it follows that

$Re\,i w^2(c) = Re\,i w^2(-c) = 0$ and therefore $\tag{11}$

$$I'_c + I'_{-c} = 0 \quad .$$

Similarly, the total contribution due to the poles at ic and $-ic$ is

$$I'_{ic} + I'_{-ic} = Re\,\pi i \oint_{\frac{1}{2}} \left[c^2 \mp \frac{R^4}{a^2 \pm c^2} \right]\left[w^2(ic) + w^2(-ic) \right] \quad . \tag{12}$$

Since $Im\ w(ic) = Im\ w(-ic) = 0$, it follows that
$Re\ iw^2(ic) = Re\ iw^2(-ic) = 0$ and therefore

$$I'_{ic} + I'_{-ic} = 0 \quad . \tag{13}$$

The contribution to the total moment due to the simple pole at $\xi = 0$ is

$$I'_o = -Re\,\pi i \oint \lim_{\xi \to 0} \left\{ \xi\,f(\xi)\frac{1}{\xi}\left[-\left(\frac{\Gamma_1}{2\pi}\right)^2\left(\frac{2}{\xi - \xi_1} - \frac{2}{\xi - \frac{c^2}{\overline{\xi}_1}} \right) + \cdots \right] \right\} \quad .$$

Since $f(0) = 0$ (Equ. (5)),

$$I'_o = 0 \quad . \tag{14}$$

The contribution of the second order pole at $\xi = 0$ is of the identical form as Equ. (21) in Ref. 1 where $f(0) = 0$ and $f'(0) = -1$ (see Appendix A). Thus, after differentation, elimination of imaginary numbers, and collection of terms we have, as in Equ. (22) in Ref. 1,

$$I_o^2 = -Re\,\rho U e^{i\phi}\left[\Gamma_1\left(\frac{c^2}{\xi_1}-\bar\xi_1\right)-\Gamma_2\left(\frac{c^2}{\xi_2}-\bar\xi_2\right)\right]\,. \tag{15}$$

The contributions to the total moment due to the third and fourth order poles at $\xi = 0$ are

$$I_o^3 = 0 \tag{16}$$

since $f''(0)=0$ (see Appendix A), and

$$I_o^4 = 0 \tag{17}$$

since $f'''(0)=0$ (see Appendix A).

For the simple poles at $\xi = \frac{c^2}{\bar\xi_1}$ and $\xi = \frac{c^2}{\bar\xi_2}$ the contribution to the total moment is of the identical form as Equs. (25) and (26) of Ref. 1, respectively.

Finally, the remaining second order poles at $\xi = \frac{c^2}{\bar\xi_1}$ and $\xi = \frac{c^2}{\bar\xi_2}$ are similarly evaluated as Equ. (27) in Ref. 1. Expressions for f in Equs. (25) and (26) and for f' in Equ. (27) are contained in Appendix A.

The remaining singularities to be evaluated are the eight branch points ($\xi_I, \xi_{II}, ----, \xi_{VIII}$) which lie on the circle. We may conveniently choose branch cuts joining these branch points as straight line segments as shown in Fig. 4.
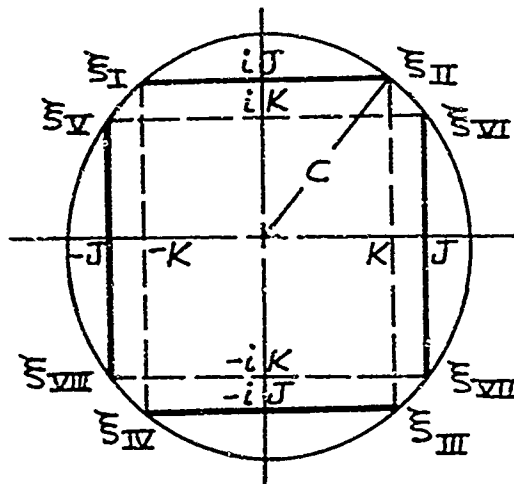
Figure 4. Branch points and branch lines of $f(\xi)$

Let us define the coordinates J and K as

$$J = \sqrt{C^2 + R^2}\big/2 \tag{18}$$

$$K = \sqrt{C^2 - R^2}\big/2 \tag{19}$$

We can enclose each branch line, e.g., ξ_I to ξ_{II} etc., with the contour ABCDEFA as shown in Figure 5.
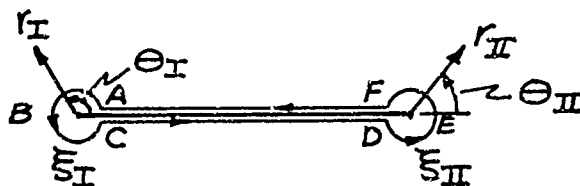

Figure 5. Branch Line Contour

Referring to equations (4) and (5), we wish to evaluate the integral

$$I_{I,II} = -Re\frac{\rho}{2}\int_{ABCDEFA} \frac{\xi}{(\xi^2+c^2)(\xi^2-c^2)}\left[\frac{\mp 4R^4\xi^4 w^2(\xi)d\xi}{\sqrt{(\xi^4+c^4)^2-4R^4\xi^4}\pm(\xi^4+c^4)}\right]$$

or

$$I_{I,II} = \pm Re\, 2\rho R^4\int_{ABCDEFA}\frac{\xi^5 w^2(\xi)d\xi}{(\xi^2+c^2)(\xi^2-c^2)\left[\sqrt{(\xi-\xi_I)\cdots(\xi-\xi_{VIII})}\pm(\xi^4+c^4)\right]}. \quad (20)$$

The evaluation of the integrals around ABC and DEF was shown to be equal to zero (see Appendix C in Ref. 1).

Using the analysis contained in Ref. 1 for the evaluation of the integrals along the lines FA and DC, we find that

$$\sqrt{(\xi-\xi_I)(\xi-\xi_{II})} = \begin{cases} i\sqrt{r_I r_{II}} & \text{on FA} \\ -i\sqrt{r_I r_{II}} & \text{on CD} \end{cases} \quad (21)$$

On FA,

$$\xi = \xi_{II} - r_{II} \quad \text{and} \quad d\xi = -dr_{II}$$

and

$$\xi - \xi_{III} = 2iJ - r_{II}$$

$$\xi - \xi_{IV} = 2\xi_{II} - r_{II}$$

$$\xi - \xi_{V} = \xi_{II} - r_{II} + (J - iK)$$

$$\xi - \xi_{VI} = \xi_{II} - r_{II} - (J + iK)$$

$$\xi - \xi_{VII} = \xi_{II} - r_{II} - (J - iK)$$

$$\xi - \xi_{VIII} = \xi_{II} - r_{II} + (J + iK)$$

(22)

Substitution of (21) and (22) into (20) gives

$$\int_{FA} = \pm Re\, Z\rho R^4 \int_0^{2K} \frac{(\xi_{II} - r_{II})^5 W^2 (\xi_{II} - r_{II})(-dr_{II})}{[(\xi_{II} - r_{II})^2 + C^2][(\xi_{II} - r_{II})^2 - C^2][i\sqrt{r_I\, r_{II}}\cdot}$$

$$\cdot (2iJ - r_{II})(2\xi_{II} - r_{II})(\xi_{II} - r_{II} + (J - iK))(\xi_{II} - r_{II} - (J + iK))\cdot$$

$$\cdot (\xi_{II} - r_{II} - (J - iK))(\xi_{II} - r_{II} + (J + iK)) \pm ((\xi_{II} - r_{II})^4 + C^4)]$$

Dropping the subscript on r_{II} and replacing r_I by $2K - r_{II}$, we have

$$\int_{FA} = \mp Re\, 2\rho R^4 \int_0^{2K} \frac{(\xi_{II}-r)^5 W^2(\xi_{II}-r)\, dr}{[(\xi_{II}-r)^2+C^2][(\xi_{II}-r)^2-C^2][i\sqrt{(2K-r)}\, r \cdot} \tag{23}$$

$$\overline{(2iJ-r)(2\xi_{II}-r)----\left(\xi_{II}-r+(J+iK)\right)\pm\left((\xi_{II}-r)^4+C^4\right)\big]}$$

Similarly, by extending the analysis along CD we find that

$$\int_{CD} = \mp Re\, 2\rho R^4 \int_{2K}^0 \frac{(\xi_{II}-r)^5 W^2(\xi_{II}-r)\, dr}{[(\xi_{II}-r)^2+C^2][(\xi_{II}-r)^2-C^2][-i\sqrt{(2K-r)}\, r \cdot} \tag{24}$$

$$\overline{(2iJ-r)(2\xi_{II}-r)-------\left(\xi_{II}-r+(J+iK)\right)}$$

$$\pm\left((\xi_{II}-r)^4+C^4\right)\big]$$

where the only change in the integral is indicated by Equ. (21). Addition of (23) and (24) yields, after algebraic reduction

$$I_{\xi_I, \xi_{II}} = \int_{FA} + \int_{CD} = \pm Re\, 4i\rho R^4 \int_0^{2K} \frac{\eta^5 h(r) W^2(\xi)\, dr}{(\eta^4-C^4)[h^2(r)+(\eta^4+C^4)^2]} \tag{25}$$

where

$$\eta(r) \equiv \xi_{II}-r = (K-r)+iJ \tag{26}$$

and

$$h(r) \equiv + \sqrt{(2K-r)r(2iJ-r)(2K+2iJ-r)(K+J+i(J-K)-r)} \cdot$$

$$\sqrt{(K-J+i(J-K)-r)(K-J+i(J+K)-r)(K+J+i(J+K)-r)}. \tag{27}$$

The same procedure is used for the evaluation of the integral around the branch cut connection ξ_{III} with ξ_{IV} and produces

$$I_{\xi_{III},\xi_{IV}} = \pm Re \, 4i \, \rho R^4 \int_0^{2K} \frac{\bar{\eta}^5 \bar{h}(r) W^2(\bar{\eta}) dr}{(\bar{\eta}^4 - C^4)[\bar{h}^2(r) + (\bar{\eta}^4 + C^4)^2]} \tag{28}$$

where

$$\bar{\eta}(r) = \xi_{III} - r = (K-r) - iJ \tag{29}$$

and

$$\bar{h}(r) = + \sqrt{(2K-r)r(-2iJ-r)(2K-2iJ-r)(K+J-i(J+K)-r)} \cdot$$

$$\sqrt{(K-J-i(J+K)-r)(K-J-i(J-K)-r)(K+J-i(J-K)-r)}. \tag{30}$$

It should be noted that the only difference between the integrals of (25) and (28) is in the sign of iJ.

We may combine (25) and (28) to obtain

$$I_{\xi_I, \xi_{II}} + I_{\xi_{III}, \xi_{IV}} = \pm Re \, 4i\rho R^4 \int_0^{2K} \left[H w^2(\eta) + \bar{H} w^2(\bar{\eta}) \right] dr \tag{31}$$

where

$$H \equiv \frac{\eta^5 h}{(\eta^4 - c^4)\left[h^2 + (\eta^4 + c^4)^2 \right]} \tag{32}$$

and

$$\bar{H} = \frac{\bar{\eta}^5 \bar{h}}{(\bar{\eta}^4 - c^4)\left[\bar{h}^2 + (\bar{\eta}^4 + c^4)^2 \right]} \; . \tag{33}$$

It was shown in Ref. 1 (p. 30) that Equ. (31) can be modified to

$$I_{\xi_I, \xi_{II}} + I_{\xi_{III}, \xi_{IV}} =$$
$$\pm Re \, 4i\rho R^4 \int_0^{2K} \bar{H} \left[w^2(\bar{\eta}) - \bar{w}^2(\eta) \right] dr \; . \tag{34}$$

w^2 is given in Ref. 1 (p. 17), H by (32), η by (26), and h by (27).

The procedure used to obtain (34) is now used to evaluate the contribution to the rolling moment due to the four remaining branch points ξ_V ---- ξ_{VIII}. Referring to Figures 4 and 6 we can enclose the branch cut connecting ξ_{VI} and ξ_{VII} with the Contour A'B'C'D'E'F'A'.
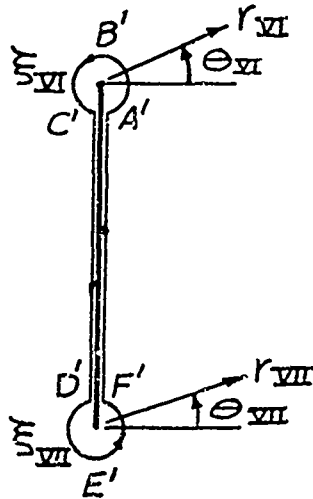
Figure 6.   Branch Line Contour

The integral we wish to evaluate is

$$I_{VII,VI} = \pm Re\, 2\oint R^4 \int_{A'B'C'D'E'F'} \frac{\xi^5 w^2(\xi)\, d\xi}{(\xi^2+C^2)(\xi^2-C^2)\left[\sqrt{(\xi-\xi_I)----(\xi-\xi_{VIII})} \pm (\xi^4+C^4)\right]} \ . \tag{35}$$

Now, we may use the polar coordinates

$$\xi - \xi_{VI} \equiv r_{VI}\, e^{i\Theta_{VI}} \tag{36a}$$

$$\xi - \xi_{VII} \equiv r_{VII}\, e^{i\Theta_{VII}} \tag{36b}$$

where both Θ_{VI} and Θ_{VII} are allowed to vary from $-\dfrac{\pi}{2}$ to $\dfrac{3\pi}{2}$.

On F'A', $\Theta_{VI} = -\dfrac{\pi}{2}$ and $\Theta_{VII} = \dfrac{\pi}{2}$

On C'D', $\Theta_{VI} = \dfrac{3\pi}{2}$ and $\Theta_{VII} = \dfrac{\pi}{2}$

Thus,

$$\Theta_{VI} + \Theta_{VII} = \begin{cases} 0 & \text{on F'A'} \\ 2\pi & \text{on C'D'} \end{cases}.$$

Therefore,

$$\sqrt{(\xi - \xi_{VI})(\xi - \xi_{VII})} = \sqrt{r_{VI}\, r_{VII}}\; e^{i\left(\frac{\Theta_{VI} + \Theta_{VII}}{2}\right)}$$

$$= \begin{cases} \sqrt{r_{VI}\, r_{VII}}\; e^{i0} & \text{on F'A'} \\ -\sqrt{r_{VI}\, r_{VII}} & \text{on C'D'} \end{cases}. \quad (37)$$

From (36b), along F'A' and C'D'

$$\xi = \xi_{VII} + r_{VII}\, e^{i\Theta_{VII}}$$
$$= \xi_{VII} + r_{VII}\, e^{i\pi/2}$$
$$= \xi_{VII} + i r_{VII}$$

and $d\xi = i\, dr_{VII}$.

Also, on F'A' we note that

$$\xi - \xi_{VI} = \left(\xi_{VII} + i r_{VII}\right) - \xi_{VI}$$
$$= (J - iK + ir) - (-J + iK)$$
$$= 2(J - iK) + ir$$

where $r = r_{VII}$ and similarly

$$\xi - \xi_{\text{VIII}} = J - iK + ir - (-J - iK) = 2J + ir$$

$$\xi - \xi_{\text{I}} = J - iK + ir - (-K + iJ) = J + K + ir - i(J + K)$$

$$\xi - \xi_{\text{II}} = J - iK + ir - (K + iJ) = J - K + ir - i(J + K)$$

$$\xi - \xi_{\text{III}} = J - iK + ir - (K - iJ) = J - K + ir + i(J - K)$$

$$\xi - \xi_{\text{IV}} = J - iK + ir - (-K - iJ) = J + K + ir + i(J - K) .$$

Also

$$\sqrt{r_{\text{VI}} r_{\text{VII}}} = \sqrt{(2K - r) r} .$$

Substitution of (37) into (35) gives, on F'A'

$$\int_{F'A'} = \pm \, Re Z \rho R^4 \int_0^{2K} \frac{(\xi_{\text{VII}} + ir)^5 w^2 (\xi_{\text{VII}} + ir)(idr)}{[(\xi_{\text{VII}} + ir)^2 + C^2][(\xi_{\text{VII}} + ir)^2 - C^2][\sqrt{(2K - r) r} \cdot}$$

$$\overline{\overline{(J + K + ir - i(J + K)) - - - (2J + ir)} \pm ((\xi_{\text{VII}} + ir)^4 + C^4)]} . \tag{38}$$

Similarly, on C'D', where r_{VII} varies between 2K and O

$$\int_{C'D'} = \pm Re Z \rho R^4 \int_{2K}^{O} \frac{(\xi_{\text{VII}} + ir)^5 w^2 (\xi_{\text{VII}} + ir)(idr)}{[(\xi_{\text{VII}} + ir)^2 + C^2][(\xi_{\text{VII}} + ir)^2 - C^2][-\sqrt{(2K - r) r} \cdot}$$

$$\overline{\overline{(J + K + ir - i(J + K)) - - - - (2J + ir)} \pm ((\xi_{\text{VII}} + ir)^4 + C^4)]} . \tag{39}$$

Adding (38) to (39) we obtain

$$\int_{F'A'} + \int_{C'D'} = I_{\xi_{VI}, \xi_{VII}} = \mp Re^4 i \rho K^4 \int_0^{2K} \frac{\tau^5 P(r) W^2(\tau) i dr}{(\tau^2+C^2)(\tau^2-C^2)\left[-P^2+(\tau^4+C^4)^2\right]} \qquad (40)$$

where

$$T = \xi_{VII} + ir = J - iK + ir.$$

Since $\eta = K - r + iJ$ (see Equ. (26))

then

$$T = -i\eta \qquad (41)$$

and therefore,

$$\tau^5 = -i\eta^5.$$

Also,

$$P(r) \equiv +\sqrt{(2K-r)r(J+K+ir-i(J+K))(J-K+ir-i(J+K))} \cdot \qquad (42)$$

$$\overline{(J-K+ir+i(J-K))(J+K+ir+i(J-K))(2J-2iK+ir)(2J+ir)} \quad .$$

We may also show that

$$ip = \sqrt{(i)^6}\, p = +\sqrt{(2K-r)r(i(J+K)-r+(J+K))} \cdot$$

$$\overline{(i(J-K)-r+J+K)(i(J-K)-r+K-J)} \cdot$$

$$\overline{(i(J+K)-r+K-J)(2iJ-r+2K)(2iJ-r)}$$

$$= h \qquad \text{(see Equ. (27)).}$$

Thus,
$$+h^2 = -p^2. \tag{43}$$

The same procedure is used for the branch cut connecting ξ_V with ξ_{VIII}. Replacing τ by $-\bar{\tau}$ and p by $-\bar{p}$ we thus obtain

$$I_{\xi_X, \xi_{VIII}} = \mp Re\, 4 i p R^4 \int_0^{2K} \frac{(+\bar{\tau}^5)(+\bar{p})\, w^2(-\bar{\tau})\, dr}{[(+\bar{\tau}^2)+C^2][(+\bar{\tau}^2)-C^2][-\bar{p}^2+(\bar{\tau}^4+C^4)^2]}. \tag{44}$$

If we let

$$P = \frac{+\tau^5 p}{(\tau^2+C^2)(\tau^2-C^2)[-p^2+(\tau^4+C^4)^2]} \tag{45}$$

then

$$\bar{P} = \frac{+\bar{\tau}^5 \bar{p}}{(\bar{\tau}^2+C^2)(\bar{\tau}^2-C^2)[-\bar{p}^2+(\bar{\tau}^4+C^4)^2]}. \tag{46}$$

Therefore

$$I_{\xi_{XI}, \xi_{VIII}} + I_{\xi_X, \xi_{VIII}} = \mp Re\, 4 i p R^4 \int_0^{2K} \left[P w^2(\tau) + \bar{P} w^2(-\bar{\tau}) \right] dr \tag{47}$$

or, alternatively

$$I_{\xi_{XI}, \xi_{VII}} + I_{\xi_X, \xi_{VIII}} = \mp Re\, 4 i p R^4 \int_0^{2K} P \left[w^2(-\bar{\tau}) - \bar{w}^2(\tau) \right] dr. \tag{48}$$

We have proved that

$$\tau = -i\eta \qquad \text{(see Equ. (41))}$$

and
$$-p^2 = h^2 \qquad \text{(see Equ. (43))}.$$

Substitution into Equ. (45) gives

$$P = \frac{-i\eta^5 h/i}{(-\eta^2+c^2)(-\eta^2-c^2)[h^2+(\eta^4+c^4)^2]}$$

$$= \frac{-\eta^5 h}{(\eta^2-c^2)(\eta^2+c^2)[h^2+(\eta^4+c^4)^2]} = -H \tag{49}$$

and therefore,

$$I_{\xi_{VI},\xi_{VII}} + I_{\xi_{X},\xi_{VIII}} = \pm Re\, 4i\rho R^4 \int_0^{2K} \overline{H}\left[w^2(-i\bar{\eta})-\overline{w}^2(-i\eta)\right]dr. \tag{50}$$

Adding this result to Equ. (34) will give the total moment contributed by the four branch lines

$$I_{\xi_I,\xi_{II}} + I_{\xi_{III},\xi_{IV}} + I_{\xi_{VI},\xi_{VII}} + I_{\xi_{X},\xi_{VIII}} =$$
$$\pm Re\, 4i\rho R^4 \int_0^{2K} \overline{H}\left\{\left[w^2(-i\bar{\eta})-\overline{w}^2(-i\eta)\right]\right.$$
$$\left. - \left[w^2(\bar{\eta})-\overline{w}^2(\eta)\right]\right\}dr. \tag{51}$$

In summary, the total rolling moment is the sum of the contour integrals around the singularities

$$M_o' = I_c' + I_{-c}' + I_{ic}' + I_{-ic}' + I_o' + I_o^2 + I_o^3 + I_o^4$$
$$+ I'_{c^2/\xi_1} + I'_{c^2/\xi_2} + I^2_{c^2/\xi_1} + I^2_{c^2/\xi_2} \tag{52}$$
$$+ I_{\xi_I,\xi_{II}} + I_{\xi_{III},\xi_{IV}} + I_{\xi_{VI},\xi_{VII}} + I_{\xi_{X},\xi_{VIII}} .$$

The equation for each integral in (52) is conveniently tabulated below.

Table 1

Integral	Equ. Number
$I'_c + I'_{-c} \equiv O$	(11)
$I'_{ic} + I'_{-ic} \equiv O$	(13)
$I'_o \equiv O$	(14)
I^2_o	(15)
$I^3_o \equiv O$	(16)
$I^4_o \equiv O$	(17)
$I'_{c^2/\bar{\xi}_1}$	(Ref.1, Equ.(25))
$I'_{c^2/\bar{\xi}_2}$	(Ref.1, Equ.(26))
$I^2_{c^2/\bar{\xi}_1} + I^2_{c^2/\bar{\xi}_2}$	(Ref.1, Equ.(27))
$\left. \begin{array}{l} I_{\bar{\xi}_I, \bar{\xi}_{II}} + I_{\bar{\xi}_{III}, \bar{\xi}_{IV}} \\[4pt] + I_{\bar{\xi}_{VI}, \bar{\xi}_{VII}} + I_{\bar{\xi}_V, \bar{\xi}_{VIII}} \end{array} \right\}$	(51)

The final result presented by Equ. (52) is programmed (see Section IV) to obtain numerical solutions with the use of a high speed digital computer. It is apparent, however, that results may be obtained for limiting cases. Thus, for example, if we consider that no external vortices are assumed to be present in the flow fields ($\Gamma_1 = \Gamma_2 = 0$), then Equation (15) equals zero as well as Equations (25), (26), and (27), of Ref. 1. Therefore the total sectional rolling moment in (52) is reduced to

$$M_0' = \pm Re \; 4i\rho R^4 \int_0^{2K} \overline{H} \left\{ \left[w^2(-i\overline{\eta}) - \overline{w}^2(-i\eta) \right] \right.$$

$$\left. - \left[w^2(\overline{\eta}) - \overline{w}^2(\eta) \right] \right\} dr \quad . \tag{53}$$

Using the expression for $W^2(\xi)$ in Ref. 1 we may note that

$$w^2(-i\overline{\eta}) = U^2\left(e^{-2i\phi} + \frac{2c^2}{\overline{\eta}^2} + e^{2i\phi}\frac{c^4}{\overline{\eta}^4} \right) + \frac{\gamma^2}{4\pi^2\overline{\eta}^2}$$

$$- \frac{U\gamma}{\pi}\left[\frac{e^{-i\phi}}{\overline{\eta}} + e^{i\phi}\frac{c^2}{\overline{\eta}^3} \right]$$

and

$$\overline{w}^2(-i\eta) = U^2\left(e^{2i\phi} + \frac{2c^2}{\overline{\eta}^2} + e^{-2i\phi}\frac{c^4}{\overline{\eta}^4} \right) + \frac{\gamma^2}{4\pi^2\overline{\eta}^2}$$

$$- \frac{U\gamma}{\pi}\left[\frac{e^{i\phi}}{\overline{\eta}} + e^{-i\phi}\frac{c^2}{\overline{\eta}^3} \right] \; ;$$

therefore,

$$w^2(-i\overline{\eta}) - \overline{w}^2(-i\eta) = U^2\left[\left(e^{-2i\phi} - e^{2i\phi} \right) + \frac{c^4}{\overline{\eta}^4}\left(e^{2i\phi} - e^{-2i\phi} \right) \right]$$

$$- \frac{U\gamma}{\pi}\left[\frac{1}{\overline{\eta}}\left(e^{-i\phi} - e^{i\phi} \right) + \frac{c^2}{\overline{\eta}^3}\left(e^{i\phi} - e^{-i\phi} \right) \right] \tag{54}$$

$$= -2U^2 i \sin 2\phi\left[1 - \frac{c^4}{\overline{\eta}^4} \right] + \frac{2U\gamma i \sin\phi}{\pi\overline{\eta}}\left[1 - \frac{c^2}{\overline{\eta}^2} \right] \quad .$$

By the same procedure,

$$w^2(\bar{\eta}) - \bar{w}^2(\eta) = -2U^2 i \sin 2\phi \left[1 - \frac{c^4}{\bar{\eta}^4}\right] + \frac{2U\gamma i \cos\phi}{\pi\bar{\eta}} \left[1 - \frac{c^2}{\bar{\eta}^2}\right] \cdot \quad (55)$$

After subtracting (55) from (54) and substituting the result in (53) we obtain

$$M_o' = \pm Re\, 4i\rho R^4 \int_0^{2K} \bar{H} \left[\frac{2U\gamma}{\pi\bar{\eta}} \left(1 - \frac{c^2}{\bar{\eta}^2}\right)(i\sin\phi - i\cos\phi)\right] dr$$

$$= \mp Re\, 4\rho R^4 \int_0^{2K} \bar{H} \left[\frac{2U\gamma}{\pi\bar{\eta}} \left(1 - \frac{c^2}{\bar{\eta}^2}\right)(\sin\phi - \cos\phi)\right] dr$$

or,

$$M_o' = \mp \gamma(\phi) Re \frac{8\rho R^4 U}{\pi} (\sin\phi - \cos\phi) \int_0^{2K} \frac{\bar{H}}{\bar{\eta}} \left(1 - \frac{c^2}{\bar{\eta}^2}\right) dr \ . \quad (56)$$

The expression for **H** (obtained from Equ. (49)) is now sub-
stituted in (56) to obtain the final result:

$$M_o' = \mp \gamma(\phi) Re \frac{8\rho R^4 U}{\pi} (\sin\phi - \cos\phi) \int_0^{2K} \frac{\bar{\eta}^2 \bar{h}\, dr}{(\bar{\eta}^2 + c^2)[\bar{h}^2 + (\bar{\eta}^4 + c^4)^2]} \ . \quad (57)$$
$$(\Gamma_1 = \Gamma_2 = 0)$$

(See Appendix B for a derivation of $\gamma(\phi)$)

Equation (57) may now be investigated in the fol-
lowing for two dimensional flow, in the absence of external
vortices, past certain configurations which are oriented
at a roll angle ϕ with respect to the cross flow velocity
vector U .

A simple cross configuration is obtained if we
reduce the body radius R to zero. If R=0, then it is
obvious that (57) equals zero and that this configuration

experiences zero net rolling moment at any roll angle ϕ, free stream flow density ρ and velocity U.* The other limiting case to consider is that of a finless cylinder where R=b (see Fig. 1). Because c=b (by the conformal transformation of the Z plane to the ξ plane) it is obvious that, since K=0 (see Equ. (19)), Equ. (57) equals zero since the upper limit of integration vanishes. Thus the rolling moment, M_o', for a finless cylinder is zero for this case, as expected.

---

*See Reference 5.

SECTION IV. Numerical Analysis and Digital Computer Results

The sectional rolling moment M_o' has been found (see Equ. (52)) to be a function of the following parameters:

$$M_o' = M_o' \left(b, R, \xi_1, \xi_2, \Gamma_1, \Gamma_2, f, U, \phi, \gamma \right) .$$

As is shown in Ref. 1 (Equ. (43)), M_o' may be expressed in dimensionless form where

$$C_{M_o'} \equiv C_{M_o'} \left(\frac{R}{b}, \frac{\xi_1}{R}, \frac{\xi_2}{R}, C_{\Gamma_1}, C_{\Gamma_2}, \phi, \frac{\gamma}{2\pi R U} \right) . \quad (58)$$

Equation (58) is used to obtain numerical data with the aid of a digital computer. For presentation of the computed data, however, the following changes were made in the above parameters:

(1) The reciprocal form b/R, is plotted with b used as the independent variable.

(2) Vortex positions $\frac{\xi_1}{R}$ and $\frac{\xi_2}{R}$ are presented as $|z_1|/R$ and $|z_2|/R$, respectively, which are obtained by mapping the positions in the ξ plane to the corresponding positions in the z plane.

(3) The free vortex circulation, γ , is dependent on the presence of a Kutta condition and is therefore not specified independently.

The two dimensional (rectangular) fin and vortex data used for the wind tunnel model in Ref. 3 provided the inputs to the computer program to generate numerical data. For a two dimensional fin, the total moment in dimensionless

form is defined as

$$C_{M_o} = \frac{M_o}{\frac{1}{2}\rho U^2 b^2 L}$$

where M_o = the total moment, L = the chord length.

The wind tunnel model geometry and flow conditions used for the parametric study are as follows:

b = 2.8 in.

L = 2.5 in.

R = .75 in.

U = 430 in./sec

ρ = 1.45 × 10^{-6} slugs/in.^{3}

α = 20 degrees

$\Gamma_1 = \Gamma_2$ = 285 in.^{2}/sec.

$|Z_1| = |Z_2|$ = 1.312 in. (Separated by an included angle of 36 degrees)

(It was reported by C. Wong (Ref. 3) that these vortex positions are essentially symmetric with respect to the body.)

To illustrate the vortex-fin interaction at various roll angles of interest, Fig. 7 shows the relative positions of the vortices with respect to the fins. The numerical results obtained from the computer study are shown in Figures 8-13.

(To check the validity of the above results this writer performed a hand calculation of the individual terms of Equ. (52). Except for Equ. (51), which proved difficult and time consuming to hand calculate, the results agreed to within five percent.)
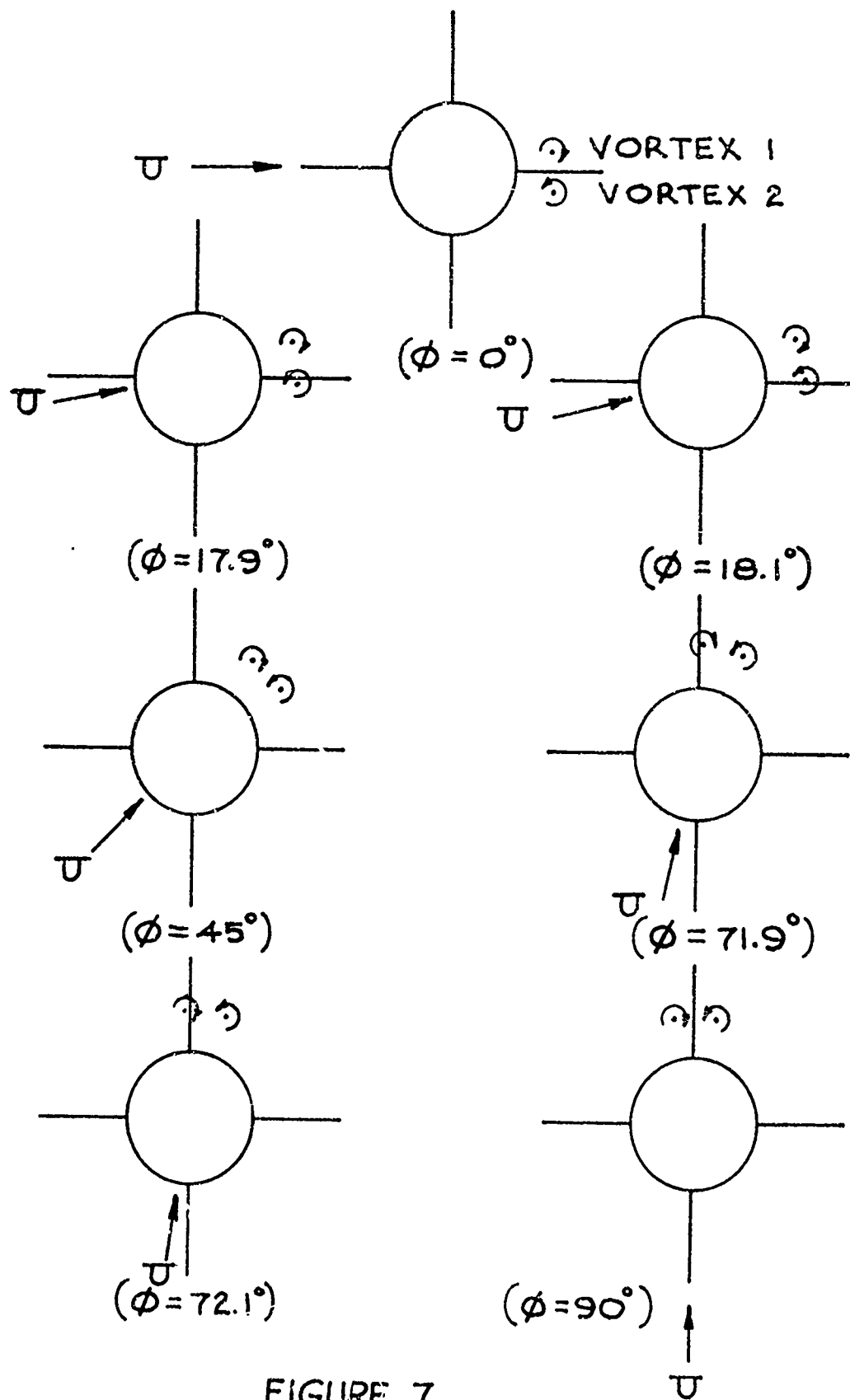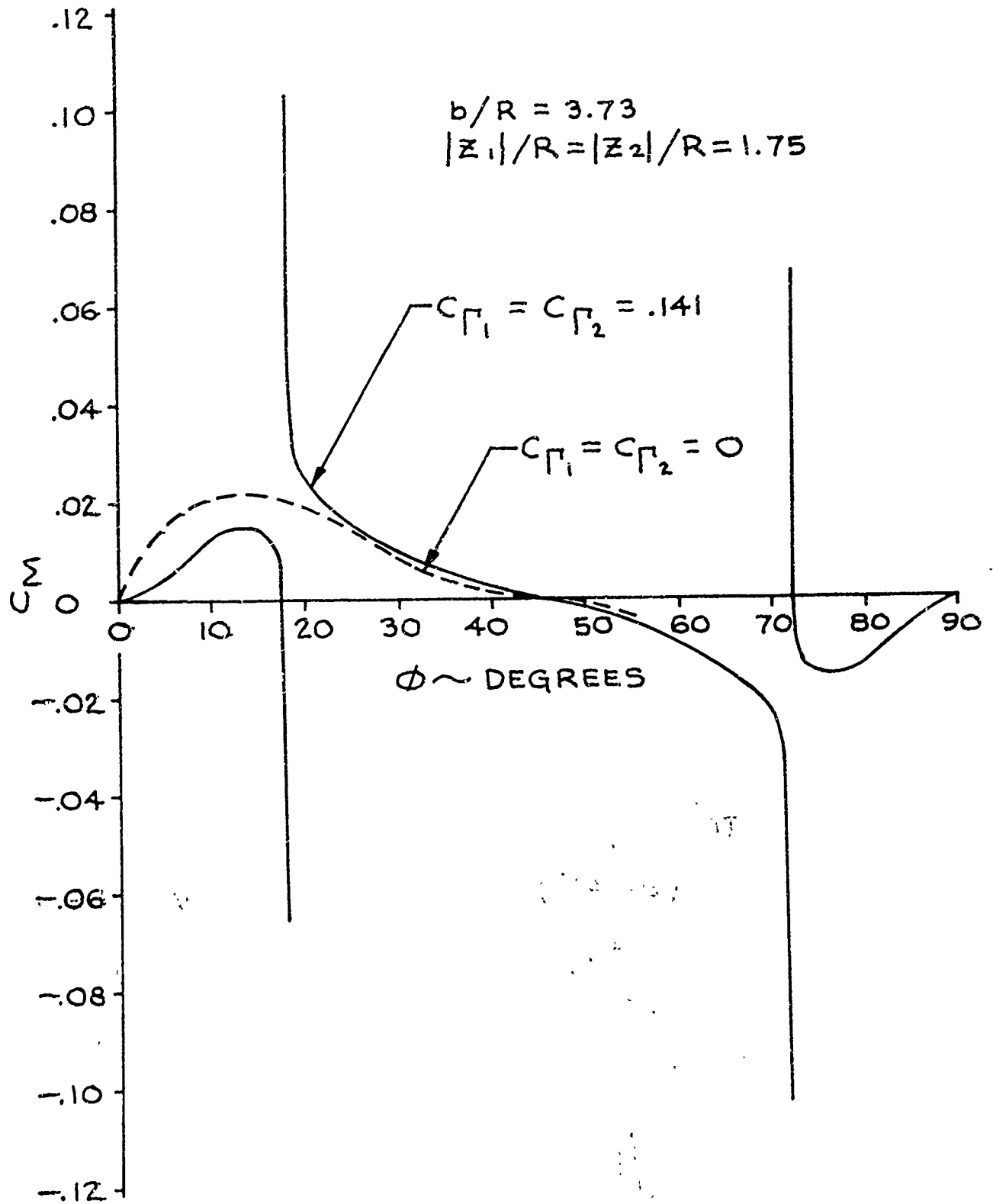
VORTEX POSITIONS IN THE Z-PLANE

FIGURE 7

C_M VS ϕ

FIGURE 8

C_M VS ϕ
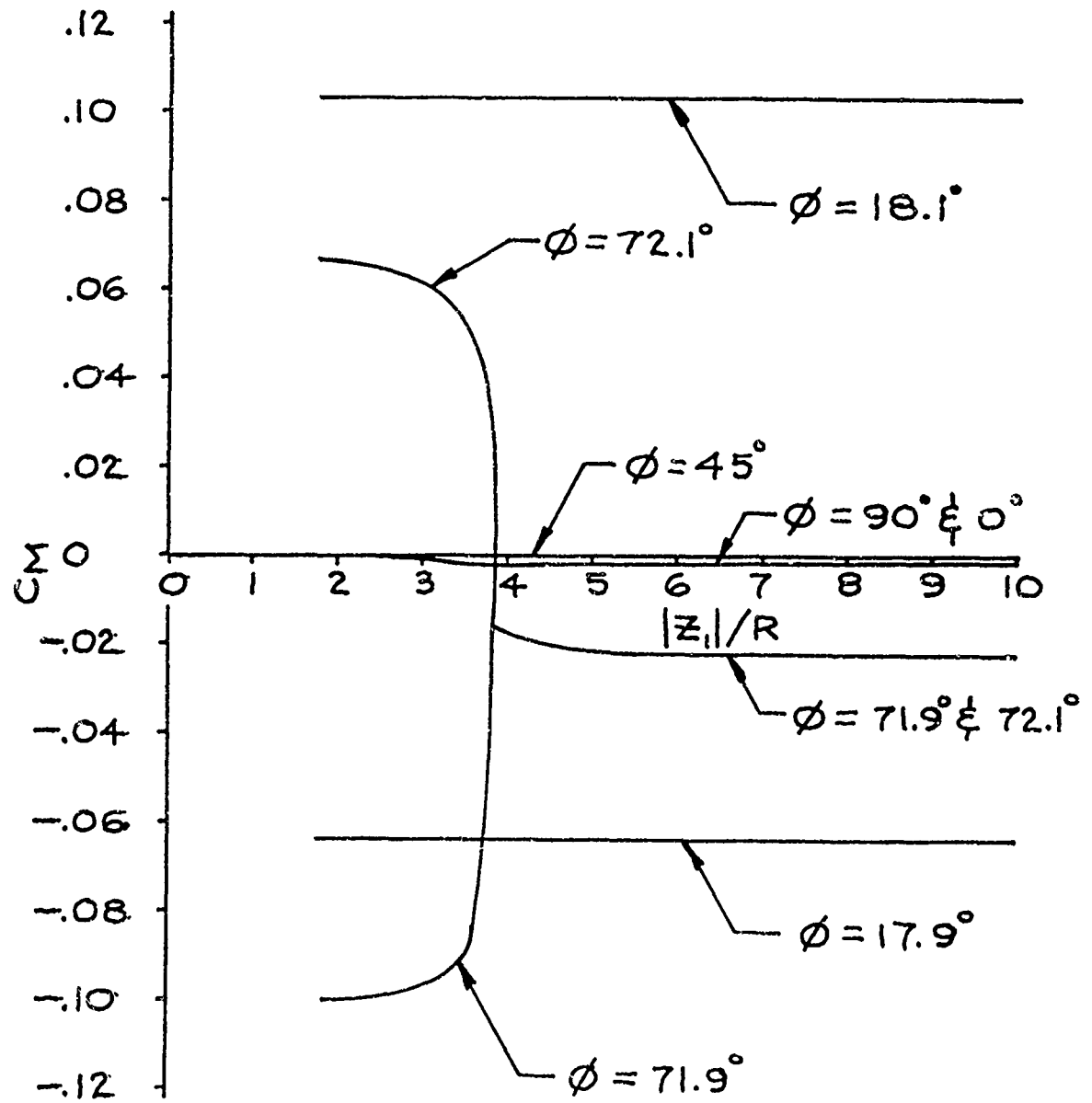
C_M vs. $|z_1|/R$

$b/R = 3.73$
$|z_1|/R = 1.75$
$C_{\Gamma_1} = C_{\Gamma_2} = .141$

FIGURE 9
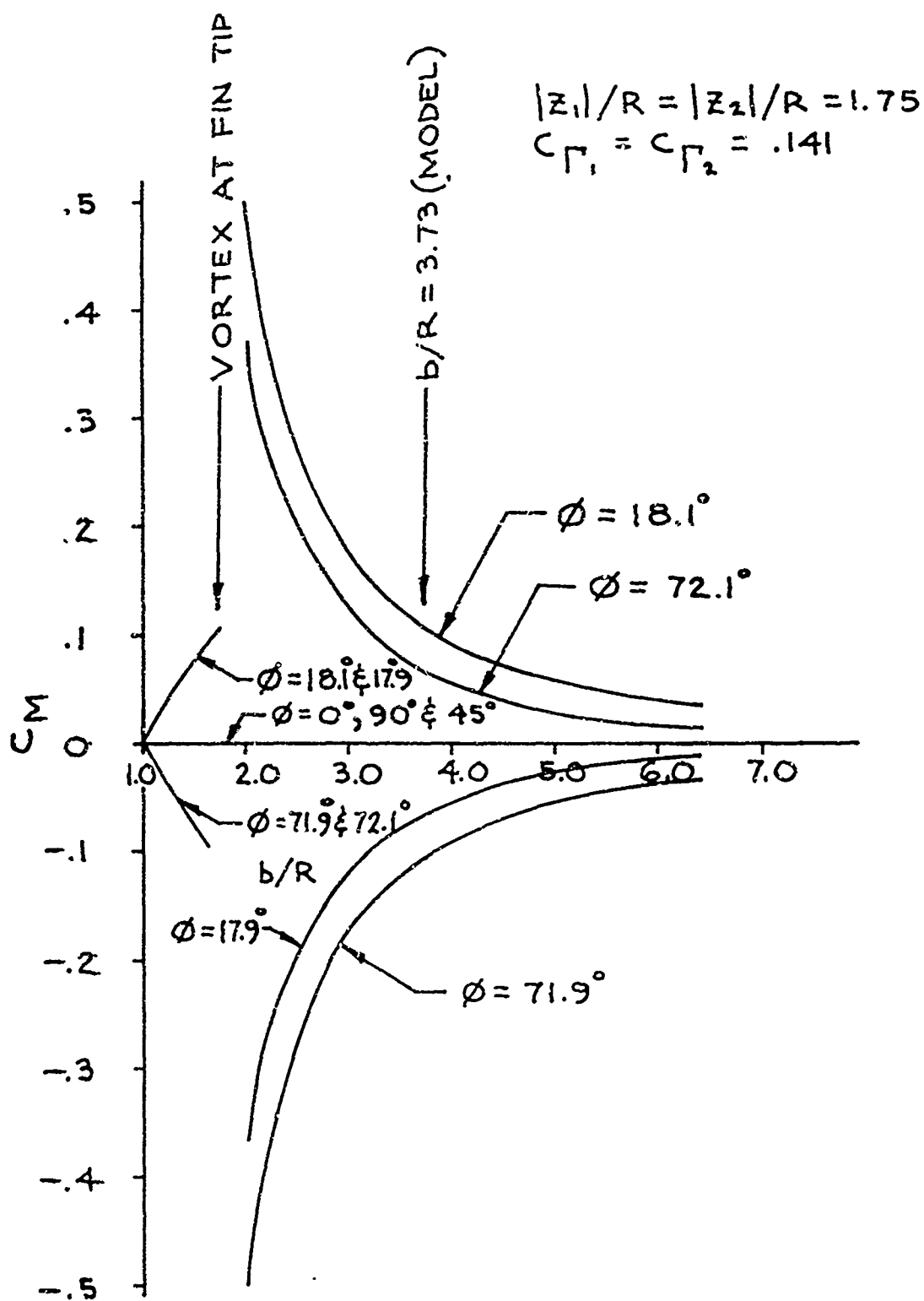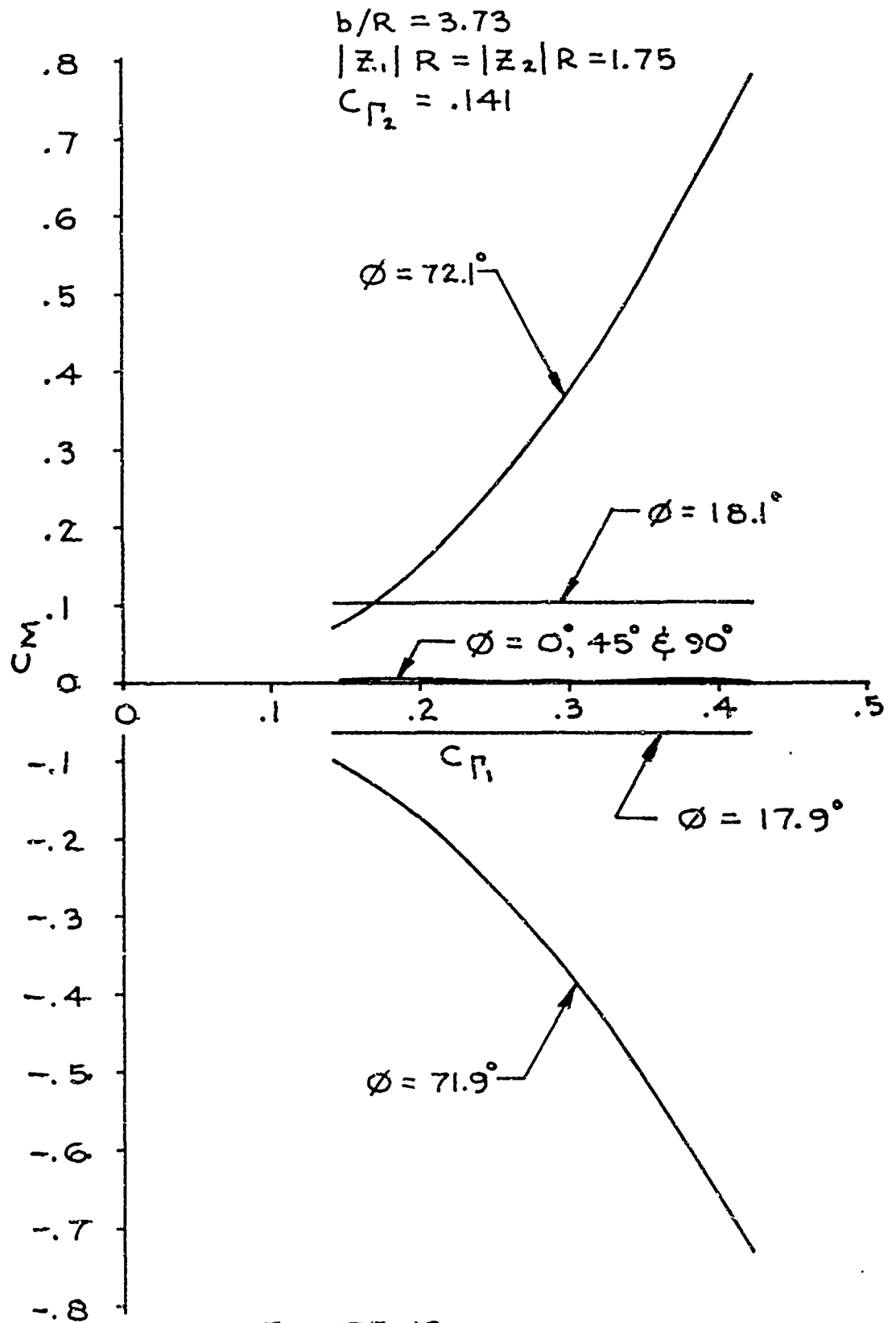
FIGURE 10

C_M VS. b/R

$|z_1|/R = |z_2|/R = 1.75$

$C_{\Gamma_1} = C_{\Gamma_2} = .141$

FIGURE 11

FIGURE 12

C_M VS. C_{Γ_2}

$b/R = 3.73$
$|z_1| R = |z_2|/R = 1.75$
$C_{\Gamma_1} = .141$

FIGURE 13

C_M VS. ϕ

FIGURE 14

C_M VS. $\emptyset$

$b/R = 3.73$

$C_{\Gamma_2} = .141$

$|Z_1|/R = |Z_2|/R = 1.75$
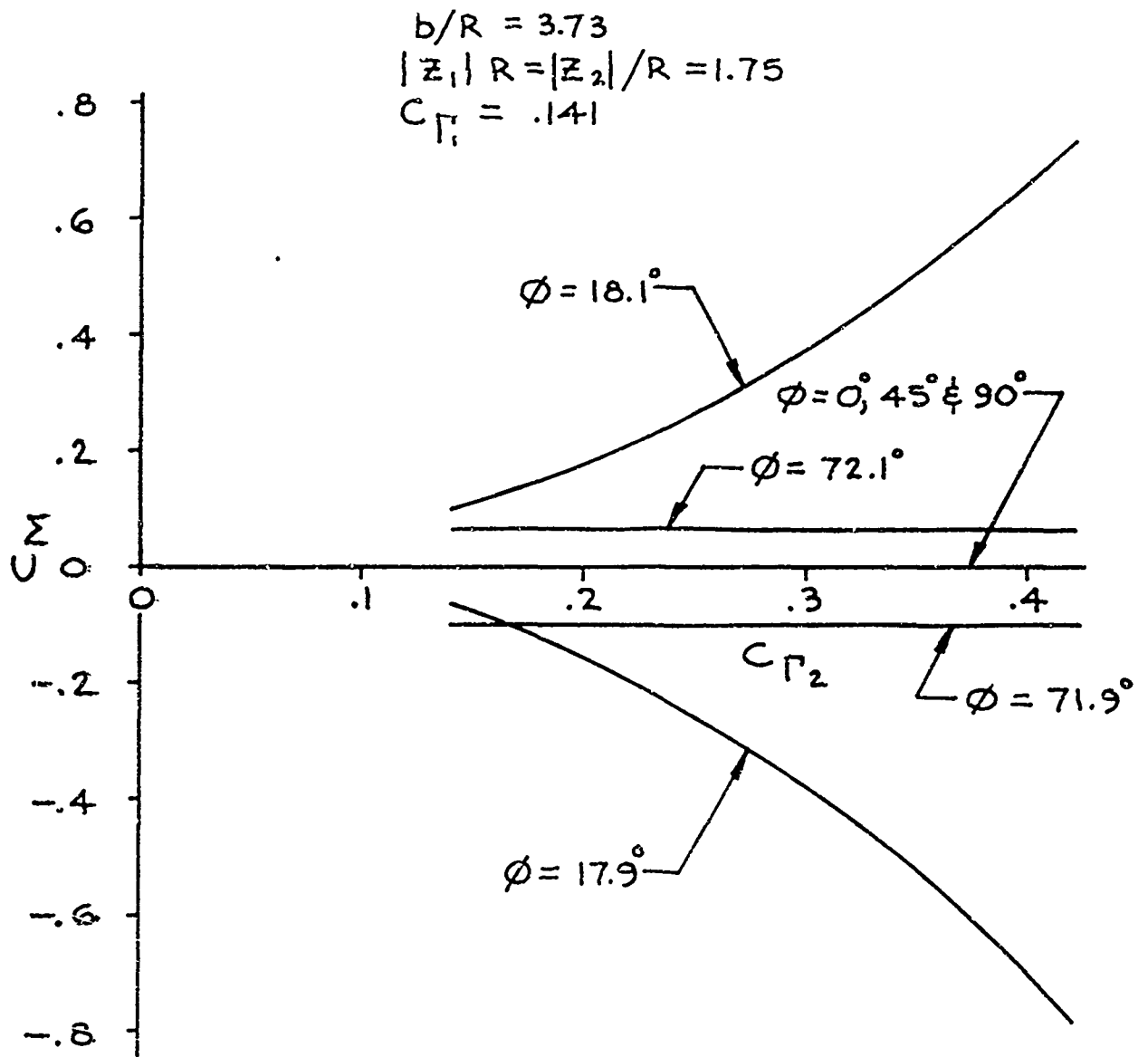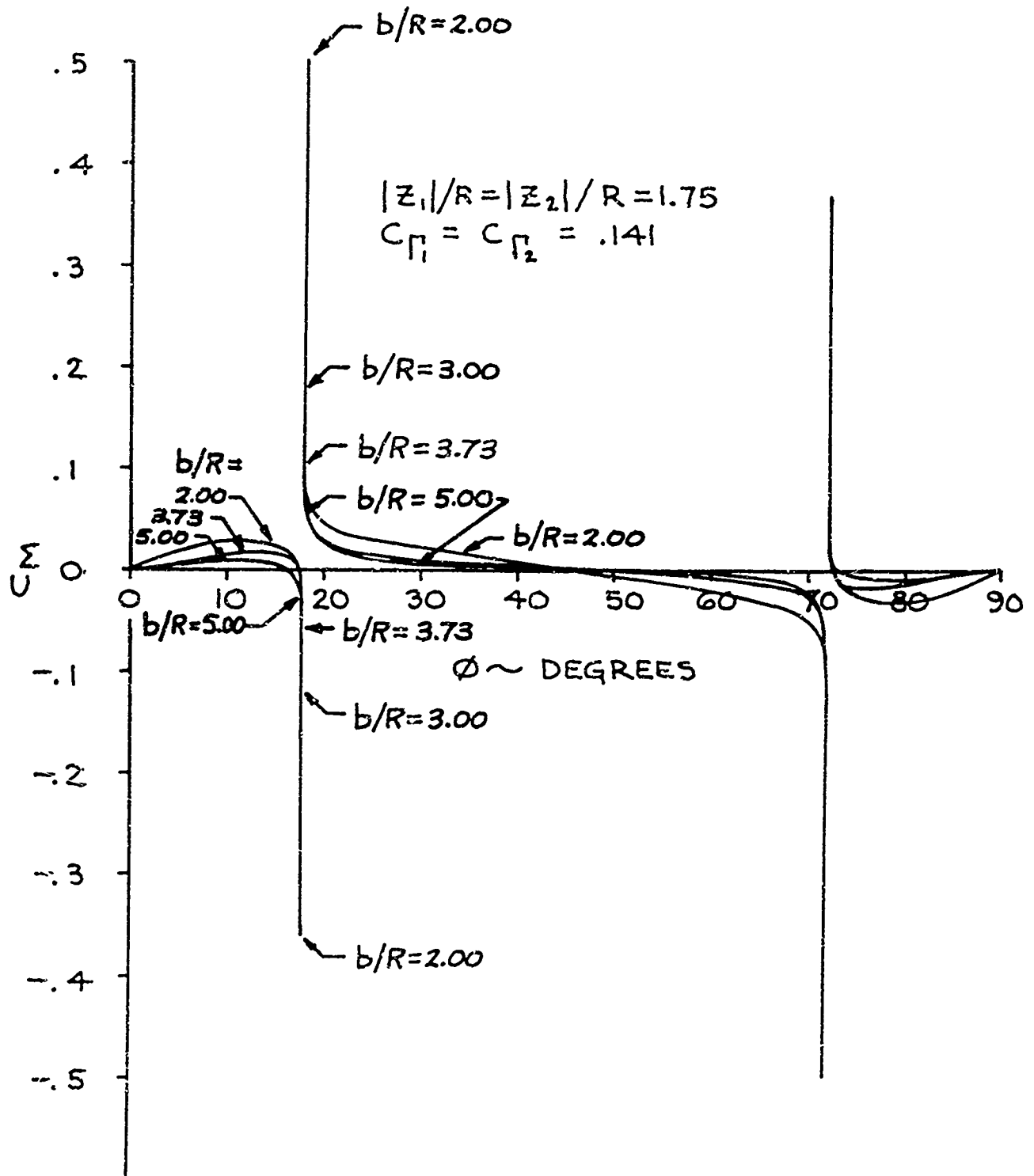
FIGURE 15
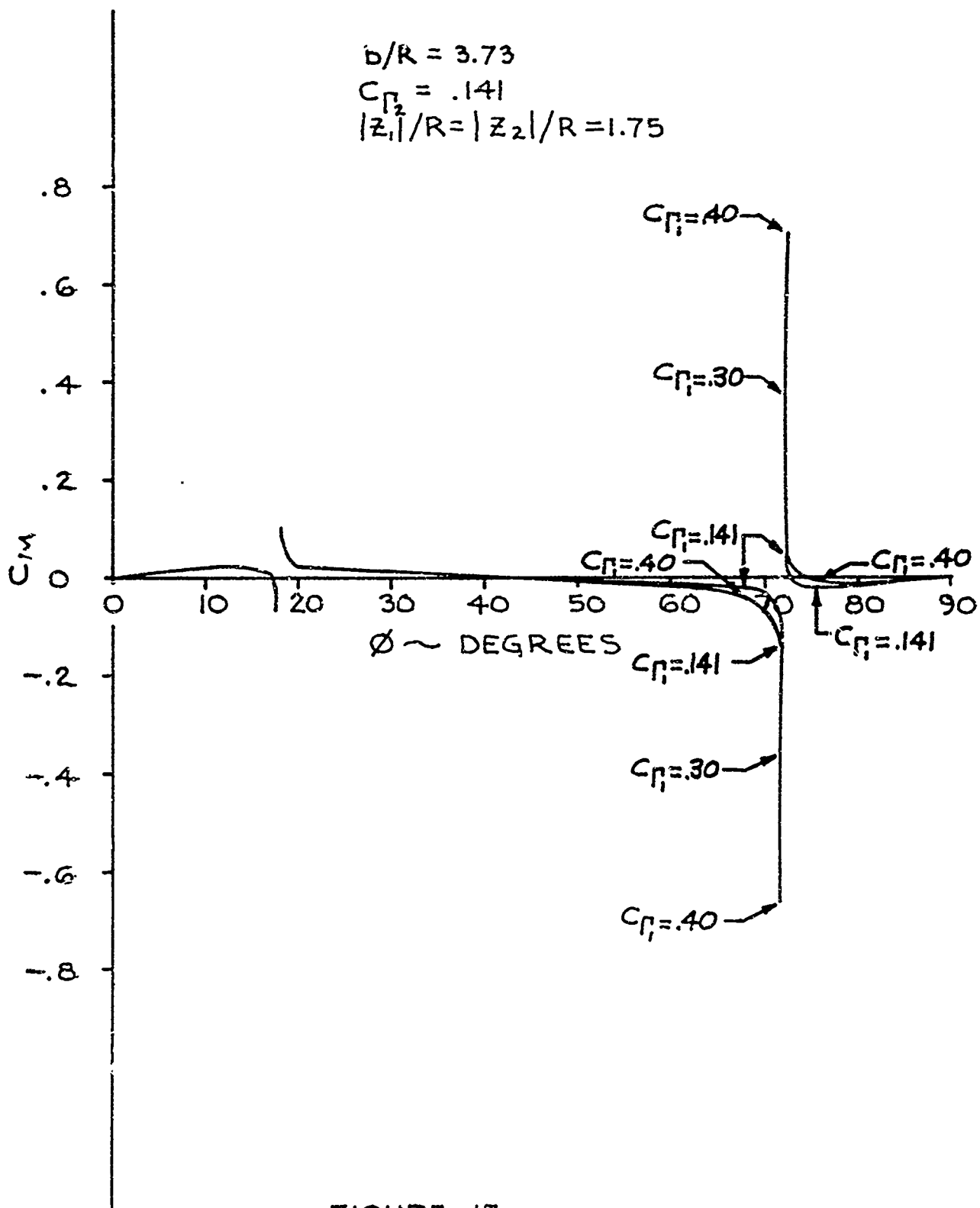
C_M VS. $\emptyset$

$b/R = 3.73$
$|Z_2|/R = 1.75$
$C_{\Gamma_1} = C_{\Gamma_2} = .141$
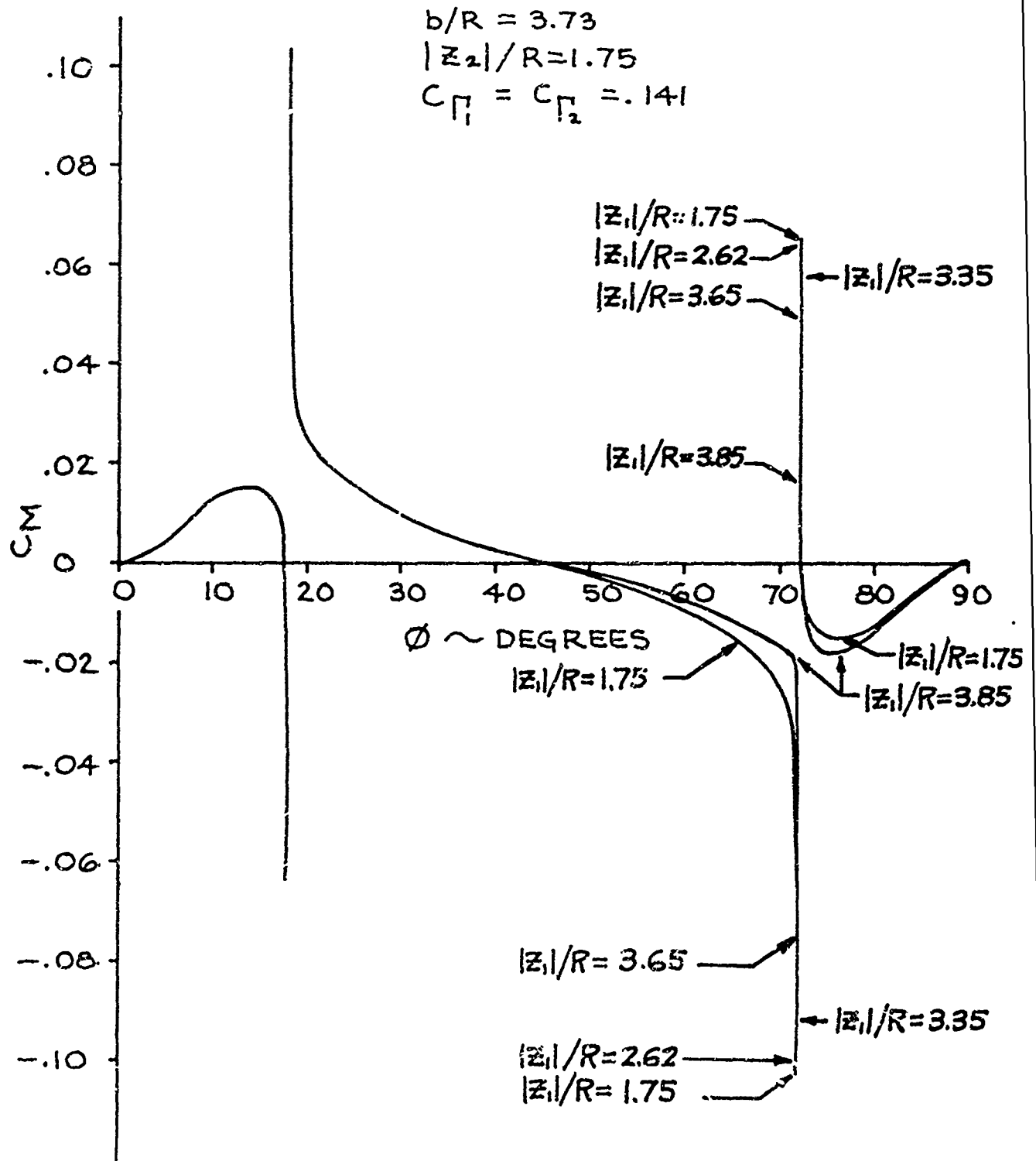
FIGURE 16

C_M VS. C_{Γ_1}

$\emptyset = 71.9°$
$b/R = 3.73$
$|Z_2|/R = 1.75$
$C_{\Gamma_2} = .141$

FIGURE 17

C_M vs. $|z_1|/R$

$$\emptyset = 71.9°$$
$$b/R = 3.73$$
$$|z_2|/R = 1.75$$
$$C_{\Gamma_2} = .141$$
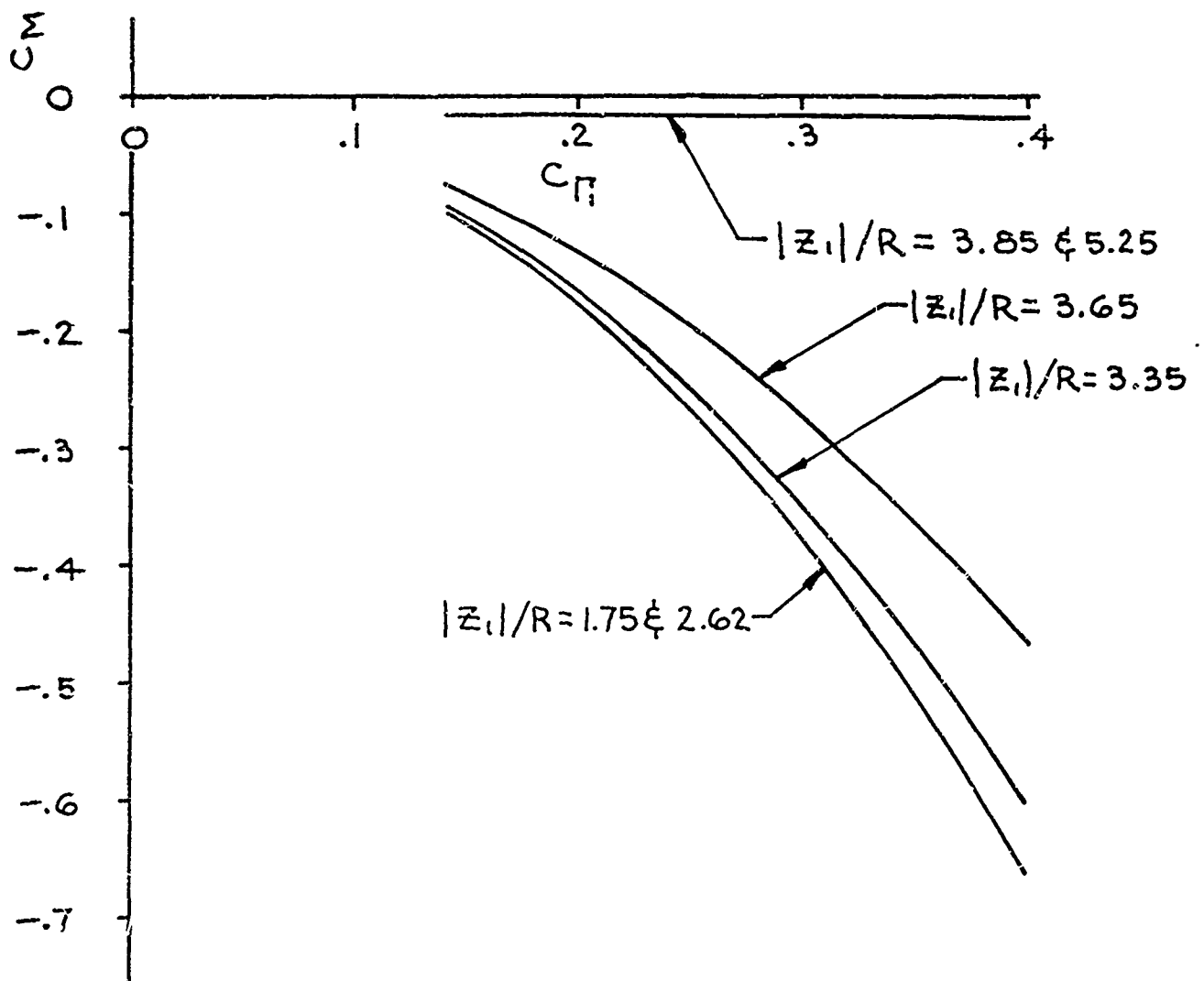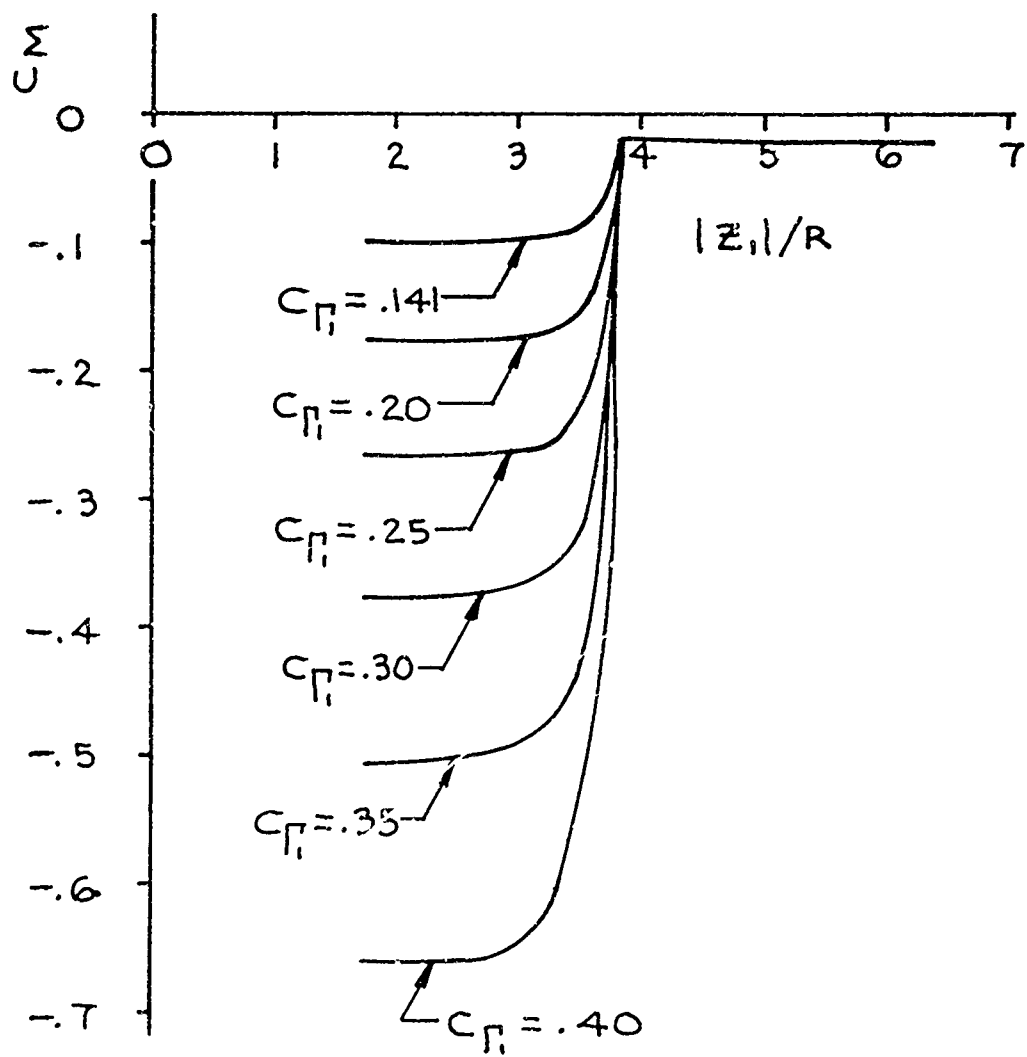
FIGURE 18

C_M VS. C_Γ

$\emptyset = 72.1°$
$b/R = 3.73$
$|Z_2|/R = 1.75$
$C_{\Gamma_2} = .141$

FIGURE 19

C_M VS. $|z_1|/R$

$\phi = 72.1°$
$b/R = 3.73$
$|z_2|/R = 1.75$
$C_{\Pi_2} = .141$

$C_{\Pi_1} = .40$

$C_{\Pi_1} = .35$

$C_{\Pi_1} = .30$

$C_{\Pi_1} = .25$

$C_{\Pi_1} = .20$

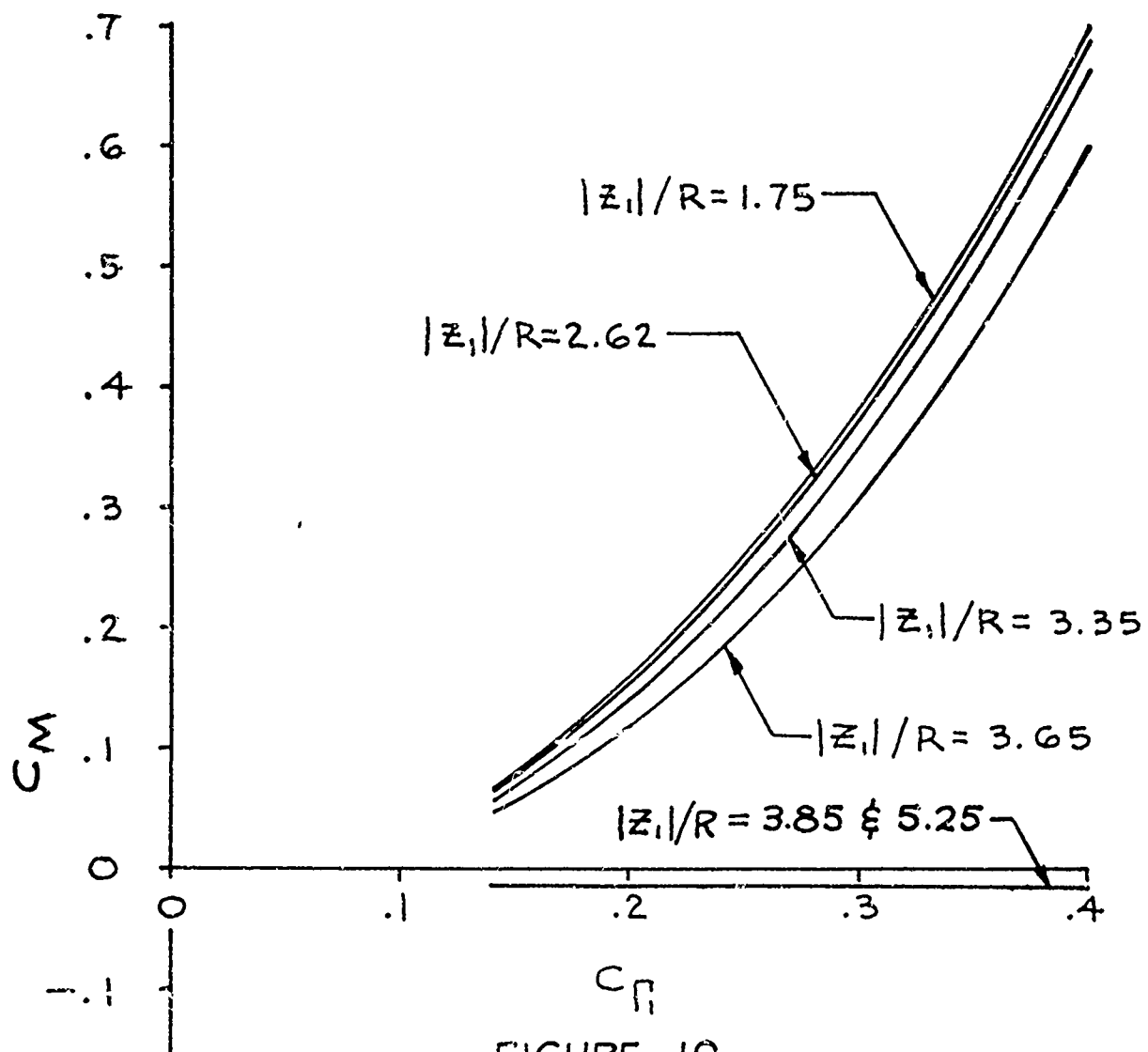$C_{\Pi_1} = .141$
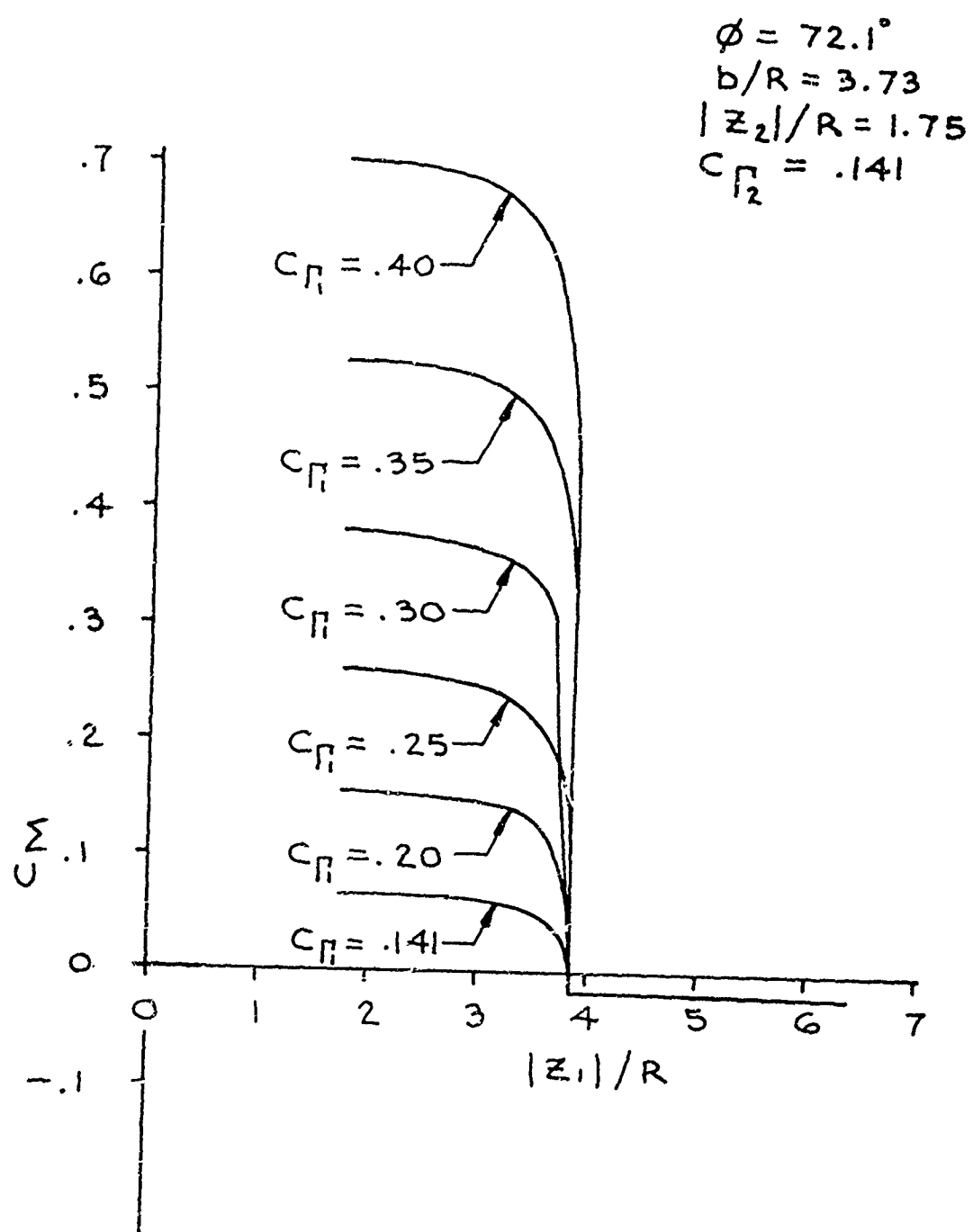
FIGURE 20

SECTION V. Conclusions

Induced rolling moments at high angles of attack are due principally to the interaction of the vortex pair generated by the body with the attached fins. It is evident that these rolling moments are strong nonlinear functions of fin span and vortex strengths and positions.

One important assumption made for this report is that the flow is two dimensional. If this restriction is removed, the problem is further complicated in that wing tip vortices as well as the body vortices must be accounted for. This is necessary as the body vortices are undoubtedly influenced by the wing tip vortex system as they pass over the fins. The resulting interaction between the vortices of both systems depends on their relative positions in the flow, relative strengths and directions of rotation. For example, two vortices of equal rotational directions will induce velocities on one another causing them to move in opposite directions , while two vortices of opposite rotations will move towards each other. The above interactions, combined with vortex-fin interaction and missile roll motions disturb the flow symmetry which would otherwise prevail if these effects did not take place.

The vortex data used for this report was obtained by experiment with the use of the subsonic wind tunnel at Boston University's College of Engineering. The preliminary data (see Section IV) indicates that the body vortices are symmetric with respect to the body, even in the vicinity of the model fins. This observation was made after reviewing photographs of the missile model and vortex geometry in the wind tunnel.

The variation of roll moment with roll angle is shown graphically in Figure 8. It is observed that, as the roll angle approaches 18 degrees, vortex 2 approaches the horizontal fin causing a rapid asymptotic increase in roll moment and stability. In the physical sense, however, the vortex may not be capable of moving so close to the fin as to cause the roll moment to approach infinite values. The interaction between the vortex and its image results in the vortex (and image) moving outboard and parallel to the fin. (The reader is referred to Reference 6 for a theoretical treatment of this interaction.) Also, the sign of the rolling moment in the vicinity of a fin depends on which side of the fin the vortex is located. In Figure 9, for example, the sign convention of the roll moment indicates that the vortex attracts the fin as it approaches it.

Figure 9 shows the sensitivity of the roll moment to perturbations made in vortex position ($|Z_i|/R$). This sensitivity is most pronounced when vortex 1 lies in close proximity to the vertical fin. In the vicinity of the vertical fin tip, the roll moment becomes highly stable when vortex 1 is to the left of the fin and highly unstable for positions to the right of the fin. (Refer to Figure 7.) The influence is less pronounced at roll angles where the vortex is located further away from the fin. A similar situation exists in Figure 10 where perturbations in position are made for vortex 2. Here, the roll moment shows greatest sensitivity when vortex 2 is in close proximity to the horizontal fin. Included in this figure is the effect of simultaneously increasing the perturbations of both vortices at $\phi = 17.9°$.

The variation of roll moment with fin span is shown in Figure 11. It is apparent that large moments exist

whenever a body vortex is located close to a fin tip. Increasing the span reduces the roll moment to an asymptotic value which indicates that the unbalanced loads inducing the roll are located near the inboard portions of the fins. It follows that for any particular condition of body vortex-fin geometry, a particular value of span will result in zero-induced rolling moment.

An almost linear variation of roll moment with perturbations in vortex strength is indicated in Figures 12 and 13. Again, the greatest variation in roll moment occurs for a vortex position close to the fin.

Results of Figures 8-13 are cross-plotted in Figures 14-20. These figures are felt to be self explanatory based on previous discussions and are therefore not described in detail.

Before analytical work is continued by including unsteady, viscous and compressible effects, it is strongly suggested that measured wind tunnel data be obtained to support the results of this report. Further, since Reference 3 does not consider stagnation point locations on the body, it is suggested that actual locations of the stagnation point be determined from experiment and compared with the theoretical locations assumed in Appendix B.

REFERENCES

1. Udelson, Daniel G., "Vortex Induced Rolling Moments on Finned Missiles at High Angle of Attack," Boston University Engineering Laboratory Report No. 1 for AFCRL (68-0569), November, 1968.

2. Mello, J.F., "Investigation of Normal Force Distributions and Wake Vortex Characteristics of Bodies of Revolution at Supersonic Speecs," Journal of the Aero/Space Sciences, Vol. 26, No. 3, pp. 155-168, March, 1969

3. Wong, C.W., "An Investigation of Vortex Path and Strength of Finned Missiles at High Angle of Attack and Numerical Calculation of Induced Rolling Moment," BUEL Report No. 2 for AFCRL (71-0092), March, 197.

4. Bryson, A.E., Jr., "Stability Derivatives for a Slender Missile with Application to a Wing-Body-Vertical-Tail Configuration," Journal of the Aeronautical Sciences, Vol. 20, No. 5, pp. 302-303, May, 1953.

5. Sacks, A.H., "Aerodynamic Interference of Slender Wing-Tail Combinations," NACA Tech. Note 3725, p. 31, January, 1957.

6. Milne-Thompson, "Theoretical Hydrodynamics," 4th Ed., MacMillan Co., pp. 358-359, 1960.

APPENDIX A

Derivatives of $f(\xi)$

The derivatives of $f(\xi)$ are listed here for reference. From Equ. (5)

$$f\left(\xi\right) = \frac{\xi}{\left(\xi^2+c^2\right)\left(\xi^2-c^2\right)} \cdot g\left(\xi\right)$$

where

$$g(\xi) \equiv \xi^4 + c^4 \mp \frac{4R^4\xi^4}{\sqrt{\left(\xi^4+c^4\right)^2 - 4R^4\xi^4} \pm \left(\xi^4+c^4\right)}$$

Hence

$$f'\left(\xi\right) = -\frac{3\xi^4+c^4}{\left(\xi^2+c^2\right)^2\left(\xi^2-c^2\right)^2} g(\xi) + \frac{\xi}{\left(\xi^2+c^2\right)\left(\xi^2-c^2\right)} g'(\xi)$$

where

$$g'(\xi) = 4\xi^3 \mp \frac{\left[\sqrt{\left(\xi^4+c^4\right)^2 - 4R^4\xi^4} + \left(\xi^4+c^4\right)\right]16R^4\xi^3 - 16R^4\xi^7\left[\frac{\xi^4+c^4-2R^4}{\sqrt{\left(\xi^4+c^4\right)^2-4R^4\xi^4}} \pm 1\right]}{\left(\xi^4+c^4\right)^2 - 4R^4\xi^4 + \left(\xi^4+c^4\right)^2 \pm 2\left(\xi^4+c^4\right)\sqrt{\left(\xi^4+c^4\right)^2-4R^4\xi^4}}$$

Also

$$f''\left(\xi\right) = \frac{12\xi^7+20c^4\xi^3}{\left(\xi^2+c^2\right)^3\left(\xi^2-c^2\right)^3} g(\xi) - 2\frac{3\xi^4+c^4}{\left(\xi^2+c^2\right)^2\left(\xi^2-c^2\right)^2} g'(\xi)$$

$$+ \frac{\xi}{\left(\xi^2+c^2\right)\left(\xi^2-c^2\right)} g''(\xi)$$

and

$$f^{?'''}(\xi) = -\frac{60\xi^{10}+264c^4\xi^6+60c^8\xi^2}{(\xi^2+c^2)^4(\xi^2-c^2)^4}\, g(\xi) + 3\,\frac{12\xi^7+20c^4\xi^3}{(\xi^2+c^2)^3(\xi^2-c^2)^3}\, g'(\xi)$$

$$-3\frac{3\xi^4+c^4}{(\xi^2+c^2)^2(\xi^2-c^2)^2}\, g''(\xi) + \frac{\xi}{(\xi^2+c^2)(\xi^2-c^2)}\, g'''(\xi) \ .$$

It is easy to show that

$$g(0) = c^4$$

and

$$g'(0) = g''(0) = 0 \ .$$

Therefore

$$f(0) = 0$$
$$f'(0) = -1$$
$$f''(0) = f'''(0) = 0 \ .$$

APPENDIX B

The purpose of this appendix is to find an analytical expression for the free vortex, γ, as well as the location of the stagnation point to satisfy the Kutta condition for the flow described by Equ. (3). The limited case will be considered where $\Gamma_1 = \Gamma_2 = 0$.

To find γ, the following procedure is used: The stagnation point is assumed to "move" with the cross flow vector, U, as it is permitted to rotate about the body. Thus, in the Z plane the stagnation point, Z_o, is located on the body contour, as follows,

$$Z_o = \begin{cases} +b & \phi = 0 \\ Re^{i(\pi + \phi)} & 0 < \phi < \pi/2 \\ -ib & \phi = \pi/2 \end{cases} \tag{59}$$

To obtain the corresponding point in the plane, we make use of the conformal mapping (see Equ. (2a))

$$\xi_o' = \pm \frac{1}{\sqrt{2}} \sqrt{\left(Z_o^2 + R^4/Z_o^2\right) \pm \sqrt{\left(Z_o^2 + R^4/Z_o^2\right)^2 - 4C^4}} \tag{60}$$

Substitution of (59) into (60) gives, for $0 < \phi < \pi/2$

$$\xi_o' = -\sqrt{R^2 \cos 2(\phi + \pi) \pm i \sqrt{C^4 - R^4 \cos^2 2(\phi + \pi)}}$$

The complex velocity is obviously zero at a stagnation point. Therefore, if we first differentiate Equ. (3) to obtain $W(\xi)$ (the complex velocity) and equate this result to zero, we have

$$O = \mho\left(e^{-i\phi} - e^{i\phi}\frac{c^2}{\xi^2}\right) + \frac{i\gamma}{2\pi\xi}$$

$$+ \frac{i\Gamma_1}{2\pi}\left[\frac{1}{\xi-\xi_1} + \frac{1}{\xi} + \frac{1}{\xi-c^2/\overline{\xi_1}}\right]$$

$$- \frac{i\Gamma_2}{2\pi}\left[\frac{1}{\xi-\xi_2} + \frac{1}{\xi} - \frac{1}{\xi-c^2/\overline{\xi_2}}\right].$$

After algebraic reduction we obtain the general expression

$$\gamma(\phi,\xi_o') = 2\pi\mho\left[\left(\xi_o' + \frac{c^2}{\xi_o'}\right)\sin\phi + i\left(\xi_o' - \frac{c^2}{\xi_o'}\right)\cos\phi\right]$$

$$-\Gamma_1\left(1 + \frac{\xi_o'}{\xi_o'-\xi_1} + \frac{\xi_o'}{\xi_o'-c^2/\xi_1}\right)$$

$$+\Gamma_2\left(1 + \frac{\xi_o'}{\xi_o'-\xi_2} - \frac{\xi_o'}{\xi_o'-c^2/\xi_2}\right).$$

Obviously, for the simple limited case where

$$\Gamma_1 = \Gamma_2 = 0 \quad , \text{ we have}$$

$$\gamma(\phi,\xi_o') = 2\pi\mho\left[\left(\xi_o' + \frac{c^2}{\xi_o'}\right)\sin\phi + i\left(\xi_o' - \frac{c^2}{\xi_o'}\right)\cos\phi\right].$$

To express γ as a real quantity, we can further define ξ_o' as

$$\xi_o' \equiv ce^{i\Theta_o} .$$

Substitution in the above expression gives

$$\gamma(\phi,\Theta_o) = 4\pi\mho c\left(\cos\Theta_o\sin\phi - \sin\Theta_o\cos\phi\right).$$

It is easy to show, by substitution, that γ is zero wherever flow symmetry exists about the configuration; that is where $\phi=0$, $\pi/4$ and $\pi/2$.